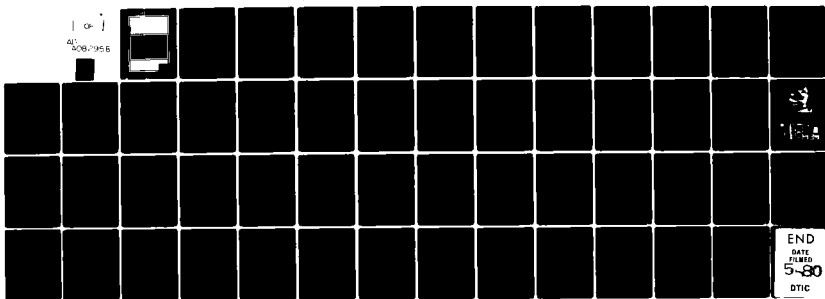AD-A082 958   ADVISORY GROUP FOR AEROSPACE RESEARCH AND DEVELOPMENT--ETC F/G 14/2
              COMPARATIVE MEASUREMENTS IN FOUR EUROPEAN WIND TUNNELS OF THE U--ETC(U)
              FEB 80   N LAMBOURNE, R DESTUYNDER, K KIENAPPEL

UNCLASSIFIED AGARD-R-673   NL

| OF |

AD
A082958

END
DATE
FILMED
5-80
DTIC

LEVEL II

AGARD-R-673

AGARD

ADVISORY GROUP FOR AEROSPACE RESEARCH & DEVELOPMENT

7 RUE ANCELLE 92200 NEUILLY SUR SEINE FRANCE

AGARD REPORT No. 673

Comparative Measurements in Four European Wind Tunnels of the Unsteady Pressures on an Oscillating Model (The NORA Experiments)

NORTH ATLANTIC TREATY ORGANIZATION

DISTRIBUTION AND AVAILABILITY
ON BACK COVER

NORTH ATLANTIC TREATY ORGANIZATION

ADVISORY GROUP FOR AEROSPACE RESEARCH AND DEVELOPMENT

(ORGANISATION DU TRAITE DE L'ATLANTIQUE NORD)

AGARD Report No.673

COMPARATIVE MEASUREMENTS IN FOUR EUROPEAN WIND TUNNELS

OF THE UNSTEADY PRESSURES ON AN OSCILLATING MODEL

(THE NORA EXPERIMENTS)

by

N.Lambourne
Royal Aircraft Establishment
Bedford MK41 6AE
United Kingdom

K.Kienappel
DFVLR-Institut für Aeroelastik
Bunsenstrasse 10
3400 Göttingen, Germany

R.Destuynder
ONERA
29 ave de la Division Leclerc
92320 Châtillon, France

R.Roos
National Aerospace Laboratory   NLR
Anthony Fokkerweg 2 –
1059 CM Amsterdam, Netherlands

THE MISSION OF AGARD

The mission of AGARD is to bring together the leading personalities of the NATO nations in the fields of science and technology relating to aerospace for the following purposes:

- Exchanging of scientific and technical information;

- Continuously stimulating advances in the aerospace sciences relevant to strengthening the common defence posture;

- Improving the co-operation among member nations in aerospace research and development;

- Providing scientific and technical advice and assistance to the North Atlantic Military Committee in the field of aerospace research and development;

- Rendering scientific and technical assistance, as requested, to other NATO bodies and to member nations in connection with research and development problems in the aerospace field;

- Providing assistance to member nations for the purpose of increasing their scientific and technical potential;

- Recommending effective ways for the member nations to use their research and development capabilities for the common benefit of the NATO community.

The highest authority within AGARD is the National Delegates Board consisting of officially appointed senior representatives from each member nation. The mission of AGARD is carried out through the Panels which are composed of experts appointed by the National Delegates, the Consultant and Exchange Programme and the Aerospace Applications Studies Programme. The results of AGARD work are reported to the member nations and the NATO Authorities through the AGARD series of publications of which this is one.

Participation in AGARD activities is by invitation only and is normally limited to citizens of the NATO nations.

PREFACE

The European GARTEUR organization initiated, a few years ago, a cooperative programme in order to obtain an understanding of the effects of the walls of a wind tunnel on the behaviour of dynamic models used for the flutter certification of aircraft.

Tests have been completed by the same team, on the same model, in four European wind tunnels and the results, collected in the same form, have been thoroughly analyzed. The output of the cooperative programme and the practical conclusions that came to light seemed so important that the Sub-Committee on Aeroelasticity of the Structures and Materials Panel proposed that a presentation should be made to an AGARD audience.

The report describes the experiments and presents the most important results; it is thought to be valuable to all the NATO community.

G.COUPRY
Chairman, Sub-Committee
on Aeroelasticity

CONTENTS

COMPARATIVE MEASUREMENTS IN FOUR EUROPEAN WIND TUNNELS OF THE UNSTEADY PRESSURES ON AN OSCILLATING MODEL (THE NORA EXPERIMENTS)*

N Lambourne (RAE)   K Kienappel (DFVLR)
R Destuynder(ONERA)   R Roos   (NLR)

SUMMARY   October 1979

To obtain experience of the influence of tunnel wall interference on flutter and other unsteady tests in transonic wind tunnels, a programme of oscillatory pressure measurements was repeated in four tunnels namely:

    3ft RAE Bedford,   S2 ONERA Modane,
    1M DFVLR Göttingen,   HST NLR Amsterdam.

These tunnels differ in the size of working section, their cross-section areas ranging from approximately 0.6 to 3.2 m^2; they also differ in the form of wall ventilation.

In each tunnel, small amplitude harmonic oscillations were applied to the same rigid half-model of a low aspect ratio lifting surface, and chordwise distributions of the fundamental components of the oscillatory pressures were measured. Measurements were also made of the steady pressure distributions for the mean position about which the oscillations occurred. Some measurements were also made of the oscillatory pressures at a wall of each tunnel.

Stream Mach number was varied between 0.60 and 1.10, and the mean steady incidence of the model from 0° to 5.5°. Tests were made for three frequencies of oscillation, the lowest, 5Hz, being regarded as a quasi-steady variation, the others, 40Hz and 60Hz, giving values of frequency parameter, based on mean chord, between 0.3 and 0.8 depending on Mach number.

In relation to normal practice, two of the tunnels were large compared to the model. They gave results in general agreement thus suggesting that for these no serious interference effects occurred. Results from the two smaller tunnels provide examples of interference effects caused either by the tunnel-to-model size ratio being too small or by unsuitable wall ventilation characteristics. It is shown that the interference effects become more severe in the presence of mixed flow with shock waves at the model surface and when the model is at incidence developing steady lift.

The results of the comparisons, whilst unable on their own to lead to rules regarding acceptable model-to-tunnel size ratios, tend to confirm current procedure in this respect. They do, however, draw attention to a possible defect in the practice of mounting a half-model at a tunnel wall that is itself ventilated.

Separate from the subject of interference, the results from the larger tunnels form a collection of data, well-authenticated by the comparisons, which is useful to the general understanding of unsteady transonic conditions.

LIST OF SYMBOLS

b	width of tunnel working section	m''	$M''_{0.5}/L'$ (see section 14.7)
c	local chord	M	stream Mach number
$\bar{c}$	mean chord	M_L	local Mach number at model surface
f	oscillation frequency, (Hz)	Mod, Mod(X)	normalised modulus of oscillatory pressure, its chordwise distribution (see section 9)
h	height of tunnel working section		
I, I(X)	normalised imaginary component of oscillatory pressure, its chordwise distribution (see section 9)	p	steady pressure
		p', p''	real and imaginary components of oscillatory pressure
L', L''	normalised real and imaginary components of oscillatory local lift (see section 9)	$\bar{p}_w$	amplitude of oscillatory pressure at tunnel wall
M', M''	normalised real and imaginary components of oscillatory local pitching moment (see section 9)	p_t	tunnel total pressure
		R, R(X)	normalised real component of oscillatory pressure, its chordwise distribution (see section 9)
$M''_{0.5}$	M'' referred to local mid chord (see section 14.7)	s	model span (root to tip)

---

*The letters of the acronym NORA refer to the names of the organisations involved: NLR, ONERA, RAE and AVA (a branch of DFVLR).

V	stream velocity	ε	phase angle of oscillatory local lift (see section 14.7)
x	distance along chord from local leading edge	θ_1	amplitude of model oscillation (see section 9)
X	x/c chordwise position		
X'	chordwise position of real component of local lift (see section 14.7)	ϕ, $\phi(X)$	phase angle of oscillatory pressure, its chordwise distribution (see section 9).
α	angle of incidence of model		

PREFACE

The setting for the experiments was so unusual as to call for comment. The work was done under the auspices of the Group for Aeronautical Research and Technology in Europe (GARTEur). It depended on very close collaboration at working level between members of the four European organisations and made use of a transportable measuring package made-up of variously-owned pieces of equipment. Also it is necessary to make clear that the authors of this document, whose main concern has been the experimental programme and the interpretation of the results, were wholly dependent on the work of

F Lopez (ONERA)   H Stange (DFVLR)   and B L Welsh (RAE)

who formed a travelling international team and were responsible for installing and operating the measuring and data processing equipment in all the tests. For each individual tunnel-entry several persons from the host organisation played vital roles; acknowledgements to them are more appropriately left to a later section of this report.

1   INTRODUCTION

Testing in wind tunnels plays an important part in flutter prediction and prevention, particularly in the transonic region – the flow region of greatest uncertainty; it will continue to do so at least until theoretical prediction of unsteady aerodynamics is completely reliable. Furthermore, model testing is the only method available to the aero-elastician for gaining experience of actual fluttering conditions. The ability of wind tunnels to reproduce the proper aerodynamic conditions of a free atmosphere and the avoidance of large wind-tunnel interference effects are therefore of great importance. The maximum allowable model size and the validity of measurements obtained close to sonic speed both are questions that remain to be answered.

The importance of interference caused by the ventilated walls of transonic tunnels has been far from clear. Over a decade ago, the discovery that aerodynamic damping was sensitive to the amount of ventilation[1] led to a spate of experiments and theoretical work aimed at establishing the most appropriate porosity conditions for avoiding these large effects[2,3]. A little later fears of unreliable results from transonic tunnels were somewhat allayed when experiments made at the NLR produced virtually the same unsteady pressures on a model oscillating in two tunnels having quite different shapes and sizes[4]. On the other hand, more recently work by NASA, ONERA and Boeing[5] showed that appreciable interference effects could occur on transonic flutter, and again brought to the fore the effects of wall porosity. It was against this background that the present experiments were planned.

Essentially the NORA experiments have consisted of testing one and the same model in four transonic tunnels of different sizes and having different wall configurations, the objective being to gain further knowledge of the effects of tunnel interference on oscillatory measurements and thus indirectly with regard to flutter testing. Unlike previous investigations of unsteady interference, the tests have included transonic conditions in which the model is developing steady lift. As well as fulfilling the primary purpose of making comparisons between the tunnels, the experiments have yielded useful knowledge about oscillatory pressure distributions under a variety of aerodynamic conditions.

2   THE EXPERIMENTS IN OUTLINE

The experiments were made with a single model representing a realistic transonic configuration and of size somewhat "too large" for the smallest, and rather "too small" for the largest tunnel; it was oscillated as a rigid body and oscillatory pressure distributions were measured at two spanwise positions for a range of aerodynamic conditions. The unsteady measurements were always obtained with the same equipment and moreover they were always made by the same NORA team. Consideration was given to matching in the various tunnels the corresponding mean steady flow conditions about which the model was oscillated and for which the oscillatory comparisons were made.

3   THE TUNNELS

The tunnels are those normally used by the participating organisations for their oscillatory and flutter tests. They are:

3Ft	RAE Bedford	(UK)
1M	DFVLR Göttingen	(Germany)
S2	ONERA Modane	(France)
HST	NLR Amsterdam	(Netherlands)

The principal dimensions and characteristics of their working sections are shown in Fig 1. Two of the tunnels have slotted walls and two have walls perforated by inclined holes. It should be noted that for the latter, the open area ratios are based on the total area of holes measured perpendicular to the axis of the holes. Also it should be noted that the 3ft tunnel has a working-section height considerably less than its name implies. The subsequent paragraphs provide more details of the working sections and wall ventilations.

3ft Tunnel

The ventilation consists of four slots and two half slots in the corners in both roof and floor. The slots are covered by perforated metal plates in the plenum chambers which by normal standards are shallow.

1M Tunnel

All four boundaries are perforated by holes, 10mm dia, drilled at $60°$ to the normal to the surface. The holes are in rows inclined at $16.1°$ to the stream direction, so that only every fifth hole is in line. For the tests in this tunnel the model was mounted at a small solid panel set in an otherwise perforated wall, Fig 2. That was the usual condition for the tests, but a few comparisons were made with the perforations at this wall covered on the flow side by a thin membrane. This condition will be denoted as "closed side wall" (CSW). Measurements of the boundary layer at this side-wall were made in the empty tunnel for both conditions. There was some variation in the shape parameter but little change in the boundary layer thickness.

S2 Tunnel

Ventilation is provided by perforations in the roof and floor drilled at $60°$ to the normal. Behind each perforated wall is another perforated sheet which when slid along the wall produces an effective change in the wall porosity from 1% to 6%. In normal use the equivalent porosity is set according to Mach number as follows:

M	Porosity
0.60, 0.80	1%
0.90, 0.95	6%
1.10	1%

Most of the measurements in this tunnel were obtained with these values of porosity, but some comparative tests were made to determine the effect of changes between the maximum and minimum values.

HS Tunnel

Both roof and floor consist of five slats separated from one another by four slots and from the solid side walls by half slots.

4   THE MODEL

A model already in existence was modified for the investigation. The planform is shown in Fig 3 and additional numerical details are given in Table 1. It has a thickness-to-chord ratio of approximately 5% and a section based on a symmetrical aerofoil in the NACA 66 series but with a small updroop near the nose; it represents a horizontal tail surface. The model-to-tunnel dimension ratios are given in Table 2. The model had been constructed from aluminium alloy as an internal framework covered with top and bottom skins. It was supported by a shaft in two bearings and was oscillated as a rigid body about a swept axis by a hydraulic rotary actuator producing pure torque and giving amplitudes up to $1°$ depending on frequency. For most of the tests an amplitude of $0.5°$ was chosen. The lowest natural frequency of the mechanical system was torsion of the shaft at about 100Hz. In every tunnel the model was mounted so that its root was just clear of the tunnel side wall with a small fairing to cover the aperture, Fig 4a. Following a common practice of half-model testing, in each tunnel the wall at which the model was mounted was required to act as a reflection wall. Oscillatory pressures were measured at two spanwise positions, Sections 2 and 4 (Fig 3), by Kulite transducers installed inside the model and connected by short lengths of tubing to pressure orifices in plugs set into the surfaces. Steady pressures were measured throughout all the experiments at Sections 1, 3 and 5, and in the more recent tests also at Sections 0 and 6. Pressures were measured at both "upper" and "lower" surfaces which, to avoid any ambiguity consequent on the model inversion necessary in some of the tunnels, are identified as E (extrados) and I (intrados) respectively, the extrados being the surface that experienced the greater suction when incidence was increased. The positions of the pressure holes are listed in Table 3.

Transition bands were glued to the extrados and intrados at 5% chord. These consisted of metal tapes with castellations about 0.09mm high. However, tests made in the HST with the bands removed showed they had negligible influence on the results.

4

Six accelerometers distributed in the model were used to determine the dynamic deformation of the model during each test.

5   INSTRUMENTATION

Apart from the pressure transducers and accelerometers installed in the model, the main instrumentation making up the measurement package, Fig 4b, comprised a servo-loop to drive the hydraulic actuator and a system to analyse the transducer signals into real and imaginary Fourier fundamental components, respectively in-phase and in-quadrature with the model displacement. The actuator controlled the mean incidence as well as oscillating the model. A potentiometer attached to the model drive shaft was used to measure the mean incidence and the oscillatory motion; it also provided a phase reference for the pressure and accelerometer signals. To avoid the possibility of differences coming from the instrumentation, in every tunnel the signals were processed by the same equipment up to the stage of producing steady voltages representing the real and imaginary components. In each set of tunnel experiments these voltages were fed to a suitable "local" computer for processing and visual presentation. The storage of the processed data on disc allowed immediate on-line comparisons to be made with the results from previous tests in the other tunnels.

The calibration of the instrumentation was made as a matter of routine during the course of each tunnel experiment.

6   MEASUREMENT PHASES

The main measurements in all the tunnels consisted of oscillatory and steady pressures on the model. In some of the tests oscillatory pressures were also measured at a rail attached to either roof or floor whichever was nearest to the model's extrados (see Fig 4a). The tunnels were occupied in a series of Phases:

Phase	Tunnel	Date
1	3Ft	Jan 77
2	S2	May 77
3	3Ft	Sept 77
4	1M	Jan 78
5	HST	Aug 78
6	S2	Apr 78

The purpose of the preliminary first phase was to check the assembly of the components and the working of the system and to provide measurements which, when compared to those of Phase 3 in the same tunnel, tested repeatability.

It was originally intended that once the transducers had been installed and the skins of the model put in place, the model should remain intact throughout the comparisons. However, instrumentation failures in the early stages led to the model being opened and its surface re-smoothed on several occasions; but from Phase 4 onwards no further failures occurred and the model remained intact. A number of key conditions in the S2 tunnel were repeated in Phase 6, which chronologically preceded Phase 5. These, unlike the original measurements in S2, suffered no instrumentation failures and, for the sake of consistency, the only results from S2 that are compared with another tunnel are those obtained in Phase 6.

Unfortunately, the experimental scatter in the 3Ft results is somewhat greater than for the other tunnels, and for this tunnel, because of failures, unsteady pressures were not obtained at all the chordwise positions.

7   RANGE OF PARAMETERS

The general ranges of tunnel Mach number and model incidence covered in the tests were:

$$0.6 \leqslant M \leqslant 1.10$$
$$0 \leqslant \alpha \leqslant 5.5^\circ$$

The standard frequencies were 5, 40 and 60Hz, the results for 5Hz being regarded as representative of quasi-steady conditions. Values of frequency parameter, based on mean chord, corresponding to these frequencies are given in Table 4. Tunnel total pressure, p_t was either 0.90, 0.60 or 0.46 bar chosen for each (M, α) combination with regard to the load on the model; but as far as possible the values of total pressure remained the same between the different tunnels.

On various occasions during different tunnel phases, ancillary tests were made to check repeatability, amplitude linearity, and the influence of sampling time. From these we conclude that the main test results are not invalidated by such extraneous effects.

8   MODEL MOTION

If the model and its mounting had been perfectly rigid, the imposed sinusoidal oscillation would have been pure rotation about the design axis as shown in Fig 3. Because of flexibility, the model motion differed from this ideal, the differences depending on the frequency of oscillation and the aerodynamic loadings. Also, in principle, the precise model motion depended on the rigidity of the tunnel mountings; thus it was important to ensure that there were no large variations in the actual model motion between the different tunnels. In all the tests, the motion was monitored by the accelerometers mounted in the

model. For 40Hz in still air a nodal line lay close to the design axis, but when the model was loaded by the oscillatory aerodynamic forces the line bent towards the rear of the model as shown in Fig 5, and the magnitude of the angular motion increased slightly along the span. The general conclusion from all measurements was that for 40Hz there were no serious tunnel-to-tunnel differences in the motion.

Increasing the oscillation frequency to 60Hz led to greater divergencies from the design axis (Fig 5), and more importantly to some differences between the various tunnels.

However, some calculations made using the doublet lattice method suggest that the unsteady pressure distributions should not be too sensitive at 40Hz and 60Hz to the differences in the nodal line positions. Nevertheless a general conclusion is that whereas the 40Hz results can be considered to be quantitatively correct, those for 60Hz should be regarded as more qualitative in nature.

9   NON-DIMENSIONAL QUANTITIES

From the measured quantities

p steady pressure

p' oscillatory pressure in phase with model displacement

p'' oscillatory pressure in quadrature with model displacement

p_t tunnel total pressure

θ_1 amplitude of model angular motion measured in a fore-and-aft plane,
the data processors produced the following non-dimensional quantities which are used throughout the comparisons.

Steady Flow

M_L, local Mach number at the model as deduced from the measured steady pressures using the isentropic relation.

Oscillatory Pressure

R and I, normalised real and imaginary pressure components, where

$$R = -p'/(p_t\,\theta_1)\ \text{rad}^{-1}\ , \qquad I = -p''/(p_t\,\theta_1)\ \text{rad}^{-1}$$

Mod and ϕ, modulus and phase angle of pressure, where

$$\text{Mod} = (R^2 + I^2)^{\frac{1}{2}}\ , \qquad \phi = \tan^{-1} I/R$$

Chordwise Position

$X \equiv x/c$, where x is distance from the local leading-edge and c the local chord.

The unusual form of the non-dimensional pressures calls for an explanation. It will be noted that the quantities M_L and R and I require only one measurement relating to tunnel flow, namely tunnel total pressure, in addition to the pressure measurements made at the model. They do not depend on knowledge of tunnel Mach number or of dynamic pressure and thus do not invoke the flow calibration of the tunnel. They are equally suitable whether the comparison of oscillatory pressures is made for identical tunnel Mach numbers, or for matched steady flow conditions at the model surface (ie same M_L) but different tunnel Mach numbers.

Usually it is the chordwise distributions R(X) and I(X) that are compared one tunnel with another, but sometimes comparisons of the distributions of Mod(X) and ϕ(X) are preferable. It may be noted that R(X) and Mod(X) are steady-based quantities since they have significance for changes of steady incidence. On the other hand, I(X) and ϕ(X) are essentially unsteady quantities.

As a matter of routine during the data processing, the steady and oscillatory pressures were integrated across the chord to give local lift (strictly normal force) and moment about the local leading edge. The integrated quantities thus made available for comparison are:

Steady Section Lift and Moment

$$\text{Lift} = \int_0^1 \left[(p_I - p_E)/p_t \right] dX$$

$$\text{Moment} = \int_0^1 \left[(p_I - p_E)/p_t \right] X\ dX$$

where I and E refer to intrados and extrados respectively.

Oscillatory Chordal Lift and Moment (separate contributions from extrados and intrados)

$$L' + iL'' = \int_0^1 (R + iI)\ dX$$

$$M' + iM'' = \int_0^1 (R + iI)\ .\ X\ dX$$

A very simple numerical procedure was used for the integrations; the results should be regarded as weighted means of the pressure rather than accurate values of lift and moment.

The other quantities that feature in the presentations are:

a , mean incidence of model measured as the angle between the horizontal and a model datum, the surface of the mounting block integral with the root of the model (deg),

M , free-stream Mach number; either a nominal value or a precise reading provided by the normal tunnel instrumentation,

f , oscillation frequency, (Hz).

The conventional non-dimensional quantities C_p', C_p'', referred to free stream dynamic pressure q, can of course be readily obtained by multiplying R, and I by the value of p_t/q appropriate to the particular Mach number.

10   BASIC STEADY FLOW OVER MODEL

The distributions of local Mach number, M_L over the upper surface of the model as deduced from the steady pressure measurements in the HST are shown in Figs 6, 7, and 8 for M = 0.80, 0.90 and 0.95.

When the incidence is near to zero, for all M, there is a small region of high suction and a recompression situated close to the leading edge. With increase of incidence, for each subsonic M the high suction region extends backwards over the chord and is terminated by a steep pressure gradient - the forward recompression. For higher subsonic M this is followed by another expansion region, which for M = 0.95 is terminated by a shock wave the rear shock, in the vicinity of mid-chord. The three-dimensional nature of the flow when the model is at incidence can be seen in the isomachs of Fig 9.

Whereas there is no doubt about the existence of the rear shock, the exact nature of the flow over the more forward part of the chord is not absolutely clear. Although for some of the test conditions the local Mach numbers in this forward region are supersonic, it is not obvious that the forward recompression involves a shock wave. Certainly there is no possibility of a shock wave for M = 0.80 even at the highest incidence. It is therefore important to note that the general shape of the forward recompression remains essentially the same as M is increased up to its highest subsonic value M = 0.95. Furthermore, the high angle of sweepback of the isomachs in the forward recompression region as seen in Fig 9, suggests that a shock wave will not be present. Instead it is probable that for much of the incidence range and for all subsonic Mach numbers, a leading edge separation vortex extends across the upper surface.

In the descriptions of the oscillatory distributions to follow we shall make reference to two main features of the upper surface flow namely, the forward recompression and the rear shock. Also it will be necessary to recognise the highly three-dimensional nature of the flow when the incidence of the model is increased.

11   GENERAL DESCRIPTION OF OSCILLATORY PRESSURE DISTRIBUTIONS

Before coming to the tunnel-to-tunnel comparisons it will be helpful to identify some of the main features of the oscillatory pressure distributions that are, in some respects, common to all the tunnels. Also, it is necessary to examine the sensitivity of certain of these features to the parameters, incidence and Mach number; for without knowledge of these sensitivities, a mere comparison between tunnels could be misleading or meaningless. Later we shall return to a more detailed discussion of some of the features when we have seen the varied results from the different tunnels.

For a general description, it is most convenient to use only the results from one of the large tunnels, the HST, in which the parameter coverage was most extensive. But it should be noted here, and will be demonstrated later, that there are no large differences between this tunnel and S2, the other large one, with regard to the shapes of the oscillatory distributions.

11.1   Influence of Oscillation Frequency and Stream Mach Number for Zero Steady Lift

For non-lifting conditions the general shapes of the oscillatory pressure distributions at Sections 2 and 4 were similar. Fig 10 shows for a tunnel Mach number M = 0.80 the results from the upper surface for oscillation frequencies 5Hz, 40Hz and 60Hz. The irregularity seen in each of the distributions at 2.5% chord should be noted as it was common to all the tunnels and was present in many other cases for incidences near to zero. It is probably due to a small separation bubble close to the leading edge. Disregarding these irregularities, we note that the chordwise distributions R(X) and I(X) for the higher frequencies bear a resemblance to the classical distributions of subsonic thin-wing theory. Both R(X) and I(X) have forward peaks (respectively in the positive and negative senses) close to the leading edge; for 40Hz and 60Hz the phase angle φ varies almost linearly across the chord from a lag at the leading edge to a lead at the trailing edge. In this example for M = 0.80, the effect of an increase in frequency is as expected. The real component R(X) is hardly changed and the main effect is to increase the magnitude of the imaginary component I(X) and thereby the modulus Mod(X) and the phase φ(X).

Influence of Incidence

Sensitivity to Small Changes in M and α

11.4 Influence of Frequency for a Lifting Condition

Fig 17 shows for M = 0.90, α = 4° the effect of increasing frequency when the model is developing steady lift. As well as causing numerical increases in I(X), there are

significant effects on R(X). For Section 2E the forward peak is reduced whilst the rear peak is moved rearward and its height is increased. With regard to these changes in the rear peak, for this particular case at least, the effect of increasing frequency is remarkably similar to the effect of increasing Mach number. Thus starting from the condition M = 0.9, f = 40Hz the effect of changing frequency to 60Hz (Fig 17a) is similar to effect of changing Mach number to 0.91 (Fig 15b). Likewise the change to 5Hz bears a resemblance to the effect of decreasing Mach number to 0.89.

At Section 4E an interesting feature is the appearance of a double peak in R(X) at 60Hz.

12   TUNNEL-TO-TUNNEL COMPARISONS OF STEADY LIFT

Before comparing the oscillatory properties, it is worth briefly examining two general indicators of interference, namely the variation of steady lift with incidence and the position of the aerodynamic centre. Fig 18 shows the local lift for Sections 1 and 3 obtained by integration of the measured steady pressures. The Mach number 0.9 has been chosen as being most suitable for these comparisons because, unlike M = 0.95 with its strong shock wave, the integrations are reasonably reliable. Nevertheless, even for M = 0.90 we must bear in mind the limited accuracy of the integration procedure with only 10 steady pressure positions across the chord at each surface. Firstly we note the variations between the tunnels of the incidence for zero lift and that the difference is greatest for the two largest tunnels. The more important and striking feature of the comparisons is the similarity in lift slope for three tunnels, HST, S2 and 3Ft and the much lower slope obtained in the 1M tunnel in its usual form. However, the closed side-wall (CSW) modification to the 1M tunnel increases the lift slope and brings it more in line with that for the other tunnels.

Fig 19 shows the local pitching moment plotted against lift, the slopes of the lines representing the chordwise position of the local aerodynamic centre. Mean slopes have been obtained from the diagrams to give the local values of lift slope and aerodynamic centre set out in Table 5. This shows that the 1M tunnel in its usual condition differs from the other tunnels not only for lift slope but also for aerodynamic centre, both properties being brought more into line by the CSW modification.

A reduction in the porosity of the roof and floor of the S2 tunnel from its usual value is seen to increase the lift slope by a few percent. Apart from this small effect, the differences in lift slope and aerodynamic centre for the three tunnels, the HST, 3Ft and S2 (with the normal value of the porosity) are of the same order as the limited accuracy of the integrations.

The lift slopes have a tendency to increase with increasing incidence – a fact which appears again when we consider the oscillatory lift. For the 3Ft tunnel there is evidence of a kink in the lift curve for Section 3 between $\alpha = 2^{\circ}$ and $\alpha = 3^{\circ}$. This fact will also be of interest when the oscillatory lift is discussed.

13   STEADY FLOW MATCHING

If the basis for an oscillatory comparison were simply the same tunnel Mach number and the same model incidence there could be a difference in the steady flows which, from the outset, could lead to differences in the oscillatory characteristics as found in the experiments of Bergh and Zwaan[4]. The purpose of matching was to eliminate as far as possible such differences in the datum flow conditions. Three different methods were used for selecting the corresponding settings of tunnel Mach number and incidence in the different tunnels for which oscillatory comparisons were made. These are:

Nominal comparison (NC): Same tunnel Mach number and same incidence.

Lift match (LM): M and α adjusted to give same M_L at the trailing edge and same steady local lift at Section 3 from integrated steady pressures. This method was normally used for non-lifting cases and ended with the local lift being close to zero value.

Pressure match (PM): This was the technique used in the HST for lifting cases in attempts to reproduce the steady pressure distributions already obtained in the 1M and 3Ft tunnels. The procedure was to adjust M and α until the best match of the extrados M_L distribution was obtained. In some cases attention was concentrated on the forward recompression, in others emphasis was placed on the rear shock. It was carried out as an iterative procedure before the oscillatory tests began; it usually ended in a somewhat arbitrary compromise.

14   TUNNEL-TO-TUNNEL OSCILLATORY COMPARISONS

14.1   The Cases for Comparison

Within the general ranges of parameters, particular tunnel-to-tunnel comparisons were made for the following standard cases:

	Non lifting				Lifting	
α	M.	p_t		α	M	p_t
≈ 0	0.60	0.9 bar		4°	0.90	0.6
	0.80	0.9		5°	0.90	0.6
	0.90	0.6		5°	0.95	0.46 or 0.6
	0.95	0.6				
	1.10	0.6				

Results for 40Hz oscillations were obtained in every case, and in many cases results were also obtained for 5Hz and 60Hz. For the S2 and 1M tunnels the comparisons include the effects of modifications to the tunnel walls.

From the large number of tunnel-to-tunnel comparisons produced by the experiments only a limited number can be presented here. The aim is firstly to demonstrate the agreement between the two large tunnels; then to identify the respective areas of agreement and disagreement between, on the one hand, one large tunnel and, on the other, the medium and small tunnels. For the latter purpose it is most convenient to use the HST as the sole comparator.

The comparisons will be mainly concerned with the shapes of the chordwise distributions of oscillatory pressure, but for the particular test Mach numbers M = 0.80 and M = 0.90, consideration will also be given to certain overall chordal characteristics as represented by integrations of the pressures. The restricted number of comparisons presented in this report was selected after a consideration of practically all possible comparisons. During the general examination of results a watch was kept for two classes of disagreement. One is a disagreement in R(X) that is present for the 5Hz quasi-steady oscillation, and therefore traceable to differences in the interference on steady or quasi-steady characteristics. The other is a disagreement in an essentially unsteady characteristic, such as a difference in I(X) or a difference in the manner in which R(X) varies with frequency.

14.2 Porosity Variation in S2

In the S2 tunnel comparative tests were made with maximum and minimum values of the roof and floor porosity. Reference has already been made to the small differences in the steady lift slope for M = 0.90. Over the whole range of Mach number and incidence, it was found that the change of porosity had only a small effect on the oscillatory pressure distributions. Two examples are shown in Fig 20.

The S2 results used in the tunnel-to-tunnel comparisons were obtained with the normally used values of porosity (see Section 3).

14.3 Comparisons Between HST and S2

All the oscillatory results obtained in the S2 tunnel during Phase 6 showed good agreement with the HST in regard to the general shapes of the distributions. Figs 21, and 22 show a selection of examples obtained for nominal comparisons. Fig 21b has been chosen to refer to a condition in which the developing sonic flow leads to irregularities which are known to be sensitive to parametric conditions. Fig 22 refers to a condition in which the local steady supersonic flow is well established and the oscillatory distributions have settled into a more definite pattern. In this case, there is remarkably good agreement for Section 2E, but some disagreement over the forward part of the chord at Section 4E, which indicates that the forward recompression is slightly more ahead in the S2 tunnel.

14.4 Comparison of HST, 1M and 3Ft for Non-lifting Conditions

M = 0.60, $\alpha \approx 0$

No results are shown for this condition for which there was reasonable agreement between the tunnels except for scatter close to the leading edge.

M = 0.80, $\alpha \approx 0$

Fig 23 shows the comparisons for Sections 2E and 4E and frequency 40Hz. For the 1M tunnel the main point of disagreement is in I(X) over the forward part of the chord, the crossing point, I(X) = 0, occurring closer to the leading edge. In contrast, in the 3Ft tunnel the crossing point is more to the rear and in this tunnel another disagreement is the prominent R bulge which does not occur in the other tunnels for this Mach number; this feature is already present for the quasi-steady oscillation but worsens with increasing frequency. Although the steady M_L distributions (Fig 24) show small differences with regard to irregularities at Section 4E, they offer no obvious clues to the reason for the differences in R(X) in the 3Ft tunnel.

M = 0.90, $\alpha \approx 0$

Fig 25a shows for 40Hz and Section 2E the comparisons for the 1M tunnel. For this tunnel, in its normal condition, the main differences are the absence of a prominent R bulge and the more positive I(X) over the forward half of the chord.

However, the CSW modification reduces these differences and indeed brings I(X) into
very close agreement with that of the HST. Fig 25b shows the comparisons for the
3Ft tunnel. In this tunnel, as in the unmodified 1M, I(X) is more positive over
the forward half of the chord, but if allowance is made for scatter there is reason-
able agreement with the HST in regard to R(X). Fig 25c shows the comparisons for
Section 4E. For I(X) there are large differences over the fore-chord which, rela-
tive to the HST, are in opposite senses for the 1M and 3Ft tunnels. Again the
difference is lessened by CSW.

Fig 26 shows comparisons of the frequency effects in the three tunnels.
Qualitatively the effects of increasing frequency are the same in all three tunnels,
producing an increase in the bulge at mid-chord, but quantitatively they differ.
Whereas both the HST and the 3Ft produce a large frequency effect on R(X), the
effect in the 1M is much less, at least in the absence of the CSW modification.

M = 0.95, α = 0

For this condition, due to the occurrence of sonic velocities, all three
tunnels produce oscillatory distributions that include irregularities, Fig 27.
Because of the sensitivity to small changes, it is of interest to consider both
nominal and matched comparisons. For both a nominal (NC) and a pressure matched
(PM) comparison, the HST produces clear evidence of a shock peak in R(X) but there
is no similar evidence from either of the other tunnels, although for the 3Ft the
absence could easily be due to the gaps resulting from transducer failures. For
the 1M, although there is the possibility that a very sharp peak has been lost
between measuring positions (as inferred from Fig 16a), it seems much more likely
that no peak exists. Indeed the M_L distributions (Fig 28) for Sections 1E and 3E
show that the maximum values of M_L in the 1M tunnel are considerably less than
those in the other tunnels.

M = 1.10, α = 0

The oscillatory pressures for Section 2E are shown in Fig 29, the upper surface
M_L distributions in Fig 30. All three tunnels produce irregularities across the
chord in the oscillatory pressure distributions and for these there is little agree-
ment. However, there is agreement with regard to the general shapes of the distribu-
tion, apart from the vicinity of the trailing edge. Whereas for the HST it seems
likely that the oscillatory pressures retain a non-zero value up to the trailing-edge,
from both the 1M and 3Ft tunnels there is evidence of shock peaks ahead of the
trailing edges.

14.5 Comparisons between HST and 1M for Lifting Conditions

M = 0.80, α = 4°

Both a nominal and a pressure-matched comparison are presented. Fig 31 shows
the oscillatory distributions for Sections 2E and 4E, and Fig 32 shows the M_L dis-
tribution at sections adjacent to those at which the oscillatory pressures were
measured. It will be seen that matching significantly improved the agreement of M_L,
particularly with regard to the strength of the forward recompression. For the
oscillatory distributions it produced an improvement at Section 4E, but worsened the
comparison of I(X) at Section 2E.

M = 0.90, α = 4°

For this case, comparisons extend over four sets of results, nominal and
matched conditions in the HST, unmodified and CSW-modified conditions in the 1M.
Fig 33 shows the oscillatory, and Fig 34 the M_L distributions. The matching process
sought to achieve agreement with the unmodified 1M, not the CSW modification, and
greatest attention was paid to the strength of the forward recompression at Section
3E; this resulted in the subsequent expansion and second recompression remaining in
disagreement. However, the CSW modification brought the steady flows in the two
tunnels into much closer agreement. Fig 33 shows that the combination of pressure
matching and the CSW modification did indeed bring the oscillatory pressure distri-
butions into reasonably good agreement. The effect of a change of frequency on the
distributions in the HST for this particular (M, α) condition has already been des-
cribed, Section 11.4, Fig 17. Qualitatively the effect of frequency in the 1M tunnel
was similar. That is, the forward peak in R(X) was reduced, and near mid-span R(X)
increased with frequency.

M = 0.95, α = 5°

The oscillatory pressures are shown in Fig 35, the upper surface M_L distribu-
tions in Fig 36.

For a nominal comparison there is a large difference in the steepness of the
recompression behind the rear shock, and to achieve a reasonable matching it was
necessary to reduce the tunnel Mach number in the HST by a large amount (0.03). The
oscillatory pressure distributions in the two tunnels have the same general form
except in the vicinity of the rear shock peak which occurs at Section 2E. A broad
conclusion is that the comparisons are improved by pressure matching although
considerable differences remain over the rear of the chord. There might have been
further improvements had the CSW modification been tested for this Mach number.

14.6 Comparisons between HST and 3Ft for Lifting Conditions

For both the standard test cases, M = 0.90, α = 4° and M = 0.95, α = 5°, the 3Ft tunnel produces oscillatory pressure distributions at Section 2E that are in serious disagreement with those from the HST. It is sufficient to describe the effects of increasing incidence for only M = 0.9. Starting from a low-lift condition, Figs 37 and 38 show how this difference develops with increasing incidence. For α = 1°, R(X) is in excellent agreement, but for higher incidences there is a growing divergence. Initially as incidence is increased in both tunnels, the forward peaks in R(X) and I(X) are displaced rearwards, but for α > 3° in the 3Ft the peak moves forwards to the leading edge, and for α = 5° the distributions in that tunnel resemble those for a non-lifting condition. For Section 4E, however, there is better qualitative agreement about the general shapes of the distributions (Fig 39).

It is important to note that the kind of differences shown in Figs 37 and 38 are not dependent on frequency. Indeed, the tunnel-to-tunnel comparisons of R(X) are much the same for all three frequencies, 5Hz, 40Hz and 60Hz. From the differences occurring at Section 2E it would appear that there must be a large difference in the types of steady flow at least for that section. The steady M_L distributions presented in Fig 5? certainly show steady flow differences between the two tunnels for all the steady measuring sections (ie 1E, 3E and 5E), but when compared with Fig 34, are not so much larger than the differences for the 1M tunnel as to offer a clear explanation of the serious dissimilarity in the oscillatory pressures occurring at Section 2E. Although it is not surprising, in view of the combined effects of model incidence and large model-to-tunnel size ratio that the 3Ft should exhibit large interference effects, it is not understood why the disagreement found in the oscillatory pressures at Section 2E is much greater than is indicated by the steady pressures at Sections 1E and 3E. It seems that in the 3Ft tunnel, the steady flow at Section 2E differs from that at the other measurement sections by being critically sensitive to an increase of incidence, and that, in this respect, the 3Ft differs from the other tunnels. The conclusion is that even for only moderate incidences, the 3Ft tunnel shows serious interference effects by dramatically failing to reproduce the oscillatory pressure distributions of the HST.

14.7 Comparison of Integrated Chordal Properties

As already described in section 9, the routine integration procedure yielded values representing the local complex lift and moment contributions (ie L', L", M', M"), for extrados and intrados at each of the measurement Sections 2 and 4. The significance of the components of moment about the leading edge is not immediately obvious, and for this reason another set of quantities has been derived from the following considerations. The classical form of the real pressure distribution R(X) shows that it can readily be replaced by a lift (ie normal force) component L' acting at a certain chordwise position X'. A similar replacement for the imaginary distribution, I(X), has far less meaning for, in its classical form, the distribution consists of positive and negative contributions which may be nearly equal; it is more in the nature of a couple. For this reason it is more appropriate to replace the distribution I(X) by an imaginary moment about mid-chord, $M''_{0.5}$ and the imaginary lift L". Finally, since it is preferable to normalise both $M''_{0.5}$ and $L"$ by L' we arrive at the following four quantities:

L' real component of oscillatory lift

$X' \equiv M'/L'$, chordwise position of real component

$\varepsilon \equiv \tan^{-1}(L"/L')$, phase angle of lift

$m" \equiv M''_{0.5}/L'$, normalised imaginary component of moment about midchord

It is noted that both L' and X' are "steady-based" because they have significance for steady and quasi-steady conditions; the other quantities ε and $m"$ are essentially unsteady properties.

M = 0.80 and M = 0.90 were chosen for the comparisons. M = 0.95 was excluded because the presence of a rear shock causes large irregularities in the distribution of the oscillatory pressures and invalidates the simple integration procedure adopted. The distributions for M = 0.80 and 0.90 were less troubled in this respect. For all cases, only the upper surface contributions are compared since it is this surface that undergoes the largest and most interesting changes.

Figs 40 and 41 are for M = 0.80 and show each of the chordal properties plotted firstly against frequency for α = 0 and then against incidence for f = 40Hz. Figs 42 and 43 show in a similar manner the results for M = 0.90. The only points included for the 3Ft tunnel are those for 40Hz, but the agreement between this tunnel and the HST is sufficiently good for this frequency to assume that the agreement extends to other frequencies.

We firstly consider the variations with frequency (Figs 40 and 42). After making allowance for scatter, it appears that both of the unsteady quantities, ε and $m"$ vary approximately linearly with frequency. But it is surprising that the lines do not pass through the origin; the vertical offsets for f = 0 are indeed consistent with the anomalous single-sign pressure phase angles for the 5Hz oscillation (see Fig 10), but the reason for this remains obscure. For M = 0.80 the lift and its phase angle in the 3Ft differ markedly from those in all the other tunnels; surprisingly the agreement is better for M = 0.90. In each case, the chordal comparisons reflect the previous comparisons for R(X) and I(X). For

12

both Mach numbers,when comparison is made with the large tunnels, there is a tendency for
m" to be numerically larger in the 3Ft and less in the 1M, but the agreement in the latter
tunnel is improved by CSW. For M = 0.90, the phase angle varies only slightly with fre-
quency and the centre of the real component of lift tends to move rearwards.

The variations with incidence (Figs 39 and 41) show other aspects. For both Mach
numbers an increase in incidence leads to an important increase in the real component of
lift. For M = 0.80 there is reasonable agreement between the HST, S2 and 1M (no results
for α > 0 are available from the 3Ft). For M = 0.90 the picture is different. There is
still close agreement between the HST and S2, indeed it is assumed that the differences
which do exist indicate the order of experimental uncertainty in the integrated results.
The shaded bands have been drawn as an average and better representation of the results from
the large tunnels. For the large tunnels, the salient effects of increasing incidence are
the increase in L'; the reduction in ε (which surprisingly shows more sensitivity to inci-
dence than to frequency); and the pronounced rearward displacement of the centre of real
lift at Section 4E for α > 3°.

With increasing incidence, firstly the 3Ft and, later, the 1M fail to reproduce the
increase in L' obtained in the large tunnels, also the differences in the other properties
tend to worsen. But again we find the CSW modification goes some way to eliminating these
differences for the 1M tunnel. The large fluctuations appearing in the 3Ft results are
probably associated with the anomalous behaviour of the oscillatory pressure distributions
when incidence is increased as previously described.

The variations with incidence plotted in Figs 41 and 43 were all obtained for precise
settings, M = 0.80 or M = 0.90 and with exact values of incidence. Other results are
available from the HST for conditions which "match" each of the steady flow conditions for
α = 4° in the 1M and 3Ft tunnels; both the nominal and matched comparisons are plotted at
the right-hand sides of the diagrams. From these an interesting point emerges. Whereas
steady flow matching produced significant changes in the steady-based properties L' and X',
and indeed improved the comparisons, it produced only small changes, and no significant
improvements in the unsteady properties represented by ε and m". This suggests that the
unsteady properties are less sensitive than the steady-based properties to small changes of
M and α. On the other hand, the CSW modification in the 1M had considerable effects on both
types of quantity.

15   SUMMARY OF RESULTS

15.1 Steady-flow Matching

Except for the irregularities very close to the leading edge, or to a shock wave when
one is present, the oscillatory pressure distributions for non-lifting cases were not sensi-
tive to small changes of incidence or Mach number; thus steady-flow matched comparisons
were little different from nominal comparisons.

For lifting cases, a nominal comparison produced steady flows in the 1M and 3Ft tunnels
that differed from the flow in a large tunnel. Some improvements in the agreement between
the distributions of steady pressure could usually be obtained by the combined adjustment of
Mach number and incidence, but an improvement in one aspect would often lead to a worsening
for another. Thus, for a lifting case a complete steady pressure match was not usually
possible; there were residual differences that could not be eliminated by any further adjust-
ment of Mach number and incidence.

Nevertheless, the matching procedure usually did make some improvements to the oscilla-
tory distributions, and there is some evidence to suggest that the improvements were greater
for the steady-based properties than for the unsteady ones.

15.2 S2 Tunnel

Changing the wall porosity had only a small effect on the steady lift at high angles
of incidence, and produced no significant effects on the shapes of the oscillatory pressure
distributions. When results obtained in the S2 with its usual wall configuration were
compared with those from the HST the agreements were generally good.

15.3 1M Tunnel

For most of the tests in this tunnel the reflection wall, that is the sidewall at
which the model was mounted, was perforated like each of the other boundaries of the working
section, (see Fig 2). In this condition, the tunnel gave a much lower steady lift curve
slope than any of the other tunnels and there were significant differences in the oscilla-
tory characteristics, including lower oscillatory lift and differences in the pressure and
lift phase angles. Closing the perforations at the model wall had a large effect on both
the steady and the oscillatory properties, and generally brought the results more into line
with those from the large tunnels. Measurements in the empty tunnel showed that closing the
perforations had little effect on the thickness of the sidewall boundary layer, but there is
some doubt as to the relevance of these empty tunnel measurements to the circumstances when
the model is in place.

15.4 3Ft Tunnel

Although for non-lifting cases this, the smallest tunnel, produced oscillatory pressure
distributions which, in some cases, were in reasonable agreement with those from the larger

tunnels, it failed to reproduce correct results when incidence was increased. This interference effect appears to lead to a critical change in the type of steady flow at the upper surface at a particular spanwise position, Section 2E. Surprisingly, in view of this disagreement, the steady local lift at other spanwise locations is in reasonable agreement with that obtained in the larger tunnels.

1.5 Features Appearing in the Oscillatory Pressure Distributions

Most of the features that show tunnel-to-tunnel differences are connected with the approach to, or the development of, local supersonic flow. They are: the R-bulge, its sensitivity to frequency, and the irregularities in both the real and imaginary distributions caused by shock waves. Both the R-bulge and the peaks associated with a shock are enhanced by an increase of frequency. For instance there are examples where no shock peak is present for a quasi-steady oscillation, but one appears for a non-zero frequency.

The R-bulge, already recognised by Tijdeman[6] and originally considered to be a precursor to a shock wave, with the present model at zero incidence first becomes definite in the RST for $M = 0.9$. In all the tunnels it is more prominent at the more inboard section. Although the zero-incidence M_L distributions are almost the same in all the tunnels, the occurrence of the bulge differs from tunnel to tunnel. For frequencies up to 60Hz it is hardly discernible in the unmodified 1M. On the other hand, in the 3Ft it is clearly evident for $M = 0.7$ and can even be detected for $M = 0.6$; for these conditions the highest local Mach numbers are of course far from sonic. It thus seems that the phenomenon cannot be related solely to the local Mach number at the model surface. Possibly its occurrence depends more on the properties of the deeper flow field away from the model surface. That is, perhaps it is less closely related to near-sonic velocities at the model surface and more to the high (but not necessarily near-sonic) velocities away from the model, and to the influence the tunnel walls have on this deeper flow field. Then the more 'open' boundaries of the 1M and the closer proximity to the model of the roof and floor of the 3Ft might be the reason why these two smaller tunnels have opposite tendencies, at least up to 60Hz, in comparison to the larger RST.

Some of the above observations on the R-bulge may be explained qualitatively with the simple model of upstream propagating acoustic waves presented in reference 6. The speed with which acoustic waves, emitted from the trailing edge, propagate towards the leading edge depends very much on the amount of head wind they encounter. The higher the local Mach number the more they are retarded and, being emitted at regular intervals, the more densely spaced they become. As the spacing of the waves is a measure for the magnitude of the pressure perturbation gradient, it is clear that in these regions the level of the unsteady pressure perturbations is increased. Further, in front of such a region the retardation of the waves may show up as an increased phase lag in the $\phi(X)$ distribution. Eventually, when the local Mach number equals one, all waves coalesce upon the shock wave. In that case acoustic information emanating from the trailing edge can reach the forward part of the airfoil only if it is radiated over the top of the shock entering the supersonic flow region from above.

Generally, when moving away from the airfoil the local Mach number reduces quickly to the free stream value. This causes the acoustic waves to tend forward since the retardation is greatest near the airfoil surface. This fanning out reduces their contribution to the R-bulge. Possibly this feature may be responsible for the fact that in the 3Ft tunnel, where the gradient of the local Mach number away from the airfoil may be less steep, the R-bulge shows up earlier.

16 OSCILLATORY PRESSURES AT TUNNEL ROOF OR FLOOR

The oscillatory pressure at the roof or the floor of each tunnel was measured with a series of transducers installed in a wooden rail. Depending on the sense in which the model was mounted, the rail was attached either to the roof or to the floor whichever was adjacent to the model extrados (ie 'upper surface'). In the 1M and 8' tunnels the attachment was directly to a perforated surface, in the RST and 3Ft tunnels the rail was attached to a convenient slat. The plan position of the rail with respect to the model is shown in Fig 44a. The small difference between the position in the 1M tunnel and that in the other tunnels is not regarded as important in the interpretation of the results.

Measurements were made of the amplitude of the pressures either at with the model oscillation and these were normalised in the same manner as the model pressures. The results for the 1M and RST were attained on-line with the equipment used for analysing the model pressures, those for the 3Ft and 8' were obtained from tape recordings using other analysis equipment. It is therefore possible that small systematic differences may be present between the results using the two methods.

A general examination of the results for various test cases shows that the pressure amplitudes tend to increase, but only slightly, with oscillation frequency and to become larger when the model is set at incidence. Examples of tunnel-to-tunnel comparisons are given in Figs 44b and 44c which show distributions of the normalised pressure amplitude $(\bar{p}_w/p_t \theta_1)$ along the rail. It is noted that all the wall pressures are small in comparison with the oscillatory pressures at the model. After making allowance for the low accuracy of the measurements, the main conclusions are as follows. For $M = 0.60$ (Fig 44b) the amplitudes for the two large tunnels are in reasonable agreement and are small when compared with those occurring in the smallest tunnel, the 3Ft. Intermediate values are obtained from the 1M tunnel. In relation to the distances between the rail and the model the pressure amplitudes in the different tunnels are correctly ordered, although the shape of the distribution

in the 3Ft is different from that in the other tunnels. For this Mach number closing the perforations at the side wall of the 1M tunnel, the CSW modification has negligible effect, both for the case shown, α = 0 and for α = 4°.

For M = 0.90 (Fig 44c), the normalised pressures are larger than for M = 0.60, but the increase is reasonably consistent with the increase with M of the normalised pressures at the model. For this higher Mach number (M = 0.90), there is a general similarity between the shapes of the distribution along the rail in the different tunnels. It is interesting to note that for this Mach number the CSW modification has a large effect which is consistent with the effect it has on the model pressures and forces. It is also of interest to note that the results for the unmodified 1M tunnel are nearly the same as those for the two large tunnels. It is clear that a change in the ventilation of the side wall has a large effect on the general pressure field.

GENERAL DISCUSSION AND CONCLUSIONS

The investigation was aimed at providing experience of tunnel interference effects on unsteady oscillatory characteristics. In considering the results from the different tunnels it is assumed that any differences that cannot be accounted for by an excessive sensitivity to parametric settings are due to differences in tunnel interference. Common to all the comparisons was the half-model technique in which one side wall of the tunnel is required to act as a reflection plane. Whilst the present results cannot provide direct information about the ability of a half-model to represent correctly a complete tip-to-tip configuration, attention is drawn to this question by the effects of changes made to the side-wall ventilation in one of the tunnels.

Absence of serious interference effects in the two large tunnels

When comparing the results from the HST and S2 tunnel it must be remembered that an agreement between two tunnels is not unambiguous evidence of an absence of interference; it could mean that both tunnels were affected but to the same extent. However, the good general agreement between these two large tunnels, coupled with their different forms of roof and floor ventilation and with the insensitivity to changes of porosity made in one of them, points strongly to the conclusion that for the NORA model neither of these tunnels produced large interference effects. This gives confidence for future testing with that ratio of model-to-tunnel size.

Interference effects in the two smaller tunnels

Each of the two smaller tunnels, the 1M and 3Ft, under some conditions gave results that differed from the larger tunnels. It is reasonable to assume that these differences were caused by interference either due to the tunnel being too small or due to unsuitable wall ventilation. For both tunnels the worst interference effects on the oscillatory pressure distributions occurred when the local flow at the model was transonic or when the model was at incidence and developing steady lift. For non-lifting conditions, that were either completely subsonic or completely supersonic, the interference effects on the distributions were sometimes small.

Most of the results from the 1M tunnel were obtained with much of the reflection wall remaining perforated. For these, it is not possible to relate the respective interference effects in this tunnel and those in the 3Ft tunnel simply to the sizes of the two working sections. For instance, for the particular Mach number examined, the slope of the steady lift curve measured in the smaller tunnels when compared with the larger tunnels was too low for the 1M tunnel but in excellent agreement for the 3Ft tunnel; yet the working section area of the 1M is approximately 1.7 times that of the 3Ft.

Closing the perforations at the side wall in the 1M tunnel, the CSW modification, brought the steady lift slope much closer to the large tunnels and improved also the agreement for the oscillatory characteristics, but only a few results were obtained with this modification. If the CSW modification had been used for all the tests in the 1M tunnel it is probable that the agreement with the larger tunnels would have been generally improved*.

In spite of the good agreement between the steady lift slope in the 3Ft and that obtained in the large tunnels, interference caused serious effects on the oscillatory pressure distributions when incidence was increased away from the condition for zero-lift. It is concluded that the tunnel-to-model size ratio for the 3Ft was too small.

Effects due to interference differences in the mean steady flow. Steady flow matching

The experiments have provided abundant evidence that the oscillatory pressure distributions can be highly dependent on the steady flow over the model. Thus, interference causing tunnel-to-tunnel differences in the steady pressure distributions is naturally likely to lead to differences in the oscillatory characteristics. Broadly speaking it was found that the greater the differences in the steady pressure distributions, the greater were the differences in the oscillatory distributions.

---

*It has been known for some time that the 1M tunnel is too open for interference free testing. To overcome this problem the tunnel is presently being equipped with a slotted test section with an open area ratio of about 3%.

Attempts to eliminate tunnel-to-tunnel differences in steady flow by adjustment of tunnel Mach number and model incidence in one tunnel relative to the settings in another, were not generally successful, except for zero lift conditions under completely subsonic conditions. Nevertheless, by this means it was sometimes possible to reduce the steady differences, for example those relating to the position or strength of a shock wave, and when this was done the oscillatory characteristics also were usually in better agreement.

Unsteady interference

No example was encountered where an interference effect on an unsteady quantity was not accompanied by differences detectable under steady conditions. Thus, even when it was possible to obtain a match of the mean steady flows (for instance at zero incidence), if tunnel-to-tunnel differences occurred in the oscillatory pressure distributions for non-zero frequencies they were accompanied by differences for quasi-steady changes. However, examples were found where the differences became greater as frequency increased; these were usually associated with the approach to sonic local flow or with the presence of shock waves.

Type and amount of wall ventilation

The differences between the results from a large tunnel and those from the 1M with perforations at the reflection wall are likely to be due to the inability of a ventilated wall to act as an adequate reflection plane. But regarded more generally, the effect of closing the side-wall perforations draws attention to the role played by the type and amount of wall ventilation in reducing tunnel interference - a role which doubtless becomes more crucial as model-to-tunnel size ratio increases.

Model-to-tunnel size ratios required to avoid large interference effects

Whilst the present results cannot themselves produce any general rules about acceptable model size, they add considerably to the general experience on which judgements have to be made in practice. On the whole, they tend to confirm conventional practice. They suggest that for a model of the NORA type and size, a tunnel having a working section of about 1m² would be marginally suitable. However for a tunnel of this size it is important that the walls have appropriate ventilation characteristics.

Oscillatory measurements in transonic flow

The sensitivity of the oscillatory pressures to small parametric changes and the irregularities that were found in some of the chordwise distributions have general implications with regard to pressure measurements in transonic flow. Unless a sufficient number of measuring positions is included and an adequate range of parameters is covered, the results obtained in the presence of local sonic or supersonic flow could be misleading.

General information on unsteady transonic conditions

Distinct from the subject of tunnel interference, the measurements obtained in the large tunnels, considered to be free from large interference effects, form a collection of information useful to the understanding of unsteady transonic conditions, and of the effects of incidence. The increase in oscillatory lift that was found to occur with increasing incidence is thought to have important implications with regard to the general problem of flutter.

REFERENCES

. K C Wight. A review of slotted-wall wind-tunnel interference effects on oscillating models in subsonic and transonic flows. J. Roy. Aero. Soc. Vo5 pp670-674 (1964).

. H C Garner. Theoretical use of variable porosity in slotted tunnels for minimizing wall interference on dynamic measurements. RAE TR 71017, ARC R&M 3706 (1971).

3 A W Moore, K C Wight. An experimental investigation of wind-tunnel wall conditions for interference-free dynamic measurements. ARC R&M 3718 (1969).

4 H Bergh, B J Zwaan. Present status of unsteady aerodynamics for lifting surfaces. AGARD CP 46 (1970).

5 C L Ruhlin, R M Destuynder, H A Gregory. Some tunnel-wall effects on transonic flutter. Journal of Aircraft Vol 13 pp62 March (1975).

6 H Tijdeman. Investigations of the transonic flows around oscillating aerofoils. NLR TR 77090U (1977).

TABLE 1

Model details

span s	=	442.5mm
root chord	=	650 mm
tip chord (effective)	=	230 mm
mean chord $\bar{c}$	=	440 mm
wing area	=	0.195 m²
thickness to chord ratio	=	5%
LE sweep	=	50°
oscillation axis position	=	0.526 chord
" " sweep	=	35°

TABLE 2

Model-to-tunnel dimension ratios

Tunnel	Tunnel width, t (m)	Tunnel height, h (m)	Model s / Tunnel t	Model $\bar{c}$ / Tunnel h	$\frac{s\bar{c}}{bh}$	Blockage for zero-incidence (%)
3Ft	0.71	0.54	0.49	0.63	0.33	1.0
1X	1.00	1.00	0.44	0.44	0.19	1.0
3:	1.75	1.77	0.25	0.25	0.06	0.3
HST	1.50	1.70	0...	0.28	0.06	0.3

TABLE 3

Positions of pressure holes

Section		1	2	3	4	5	6
Spanwise position	.177	.252	.424	0.61	0.717	0.786	0.895
Pressures	Steady	Steady	Unsteady	Steady	Unsteady	Steady	Steady
A. Extrados (Upper surface)							
X =			.01	.02	.01	.075	.10
			.02	.25		.15	.15
	.05	.10	.05	.15	.05		.25
	.15	.15	.15		.15	.30	.30
				.30		.40	.40
	.50	.50		.40		.50	.50
			.25	.60			.65
			.45			.75	.75
			.65	.75	.40	.85	
				.90			
B. Intrados (Lower surface)							
X =							

TABLE 4

Values of frequency parameter, $2\pi f \bar{c}/V$

M	f = 5Hz	40Hz	60Hz
0.60	0.07	0.56	0.83
0.80	0.05	0.43	0.64
0.90	0.05	0.39	0.58
0.95	0.05	0.37	0.55
1.10	0.04	0.33	0.49

TABLE 5

Lift-curve slope and aerodynamic centre, M = 0.90
(Mean values for the incidence range from 0 to 3° greater than zero-lift angle)

Tunnel	SECTION 1		SECTION 3	
	Lift slope (scaled)*	Aerodynamic centre	Lift slope (scaled)*	Aerodynamic centre
HST	1.00	0.270c	1.11	0.217c
S2 (6% open)	0.99	0.265	1.17	0.217
S2 (1% open)	1.04	0.265	1.20	0.217
1M	0.81	0.240	0.89	0.200
1M (CSW)	0.96	0.270	1.08	0.217
3Ft	0.98	0.260	1.07	0.216

*The lift slopes shown above have been normalised by the value at
Section 1 in the HST, for which the local $dC_L/d\alpha$ = 2.96 rad⁻¹

18

RAE 3Ft Bedford

910

442·5   640
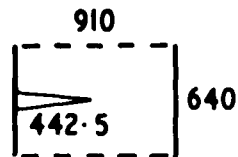
Roof & Floor : slotted 14% open

Side walls : solid

DFVLR 1M Göttingen

1000

442·5   1000
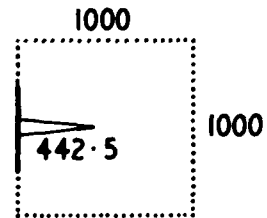
Roof & Floor : perforated 6% open

Side walls : perforated 6% open

ONERA S2 Modane

1750

442·5   1770
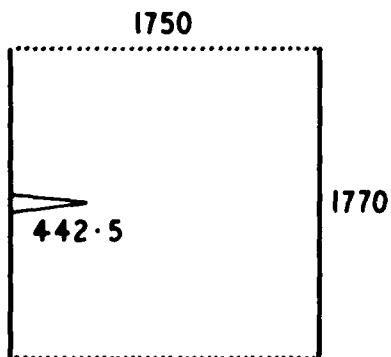
Roof & Floor : perforated 1% to 6% open

Side walls : solid

NLR HST Amsterdam

2000

442·5   1600
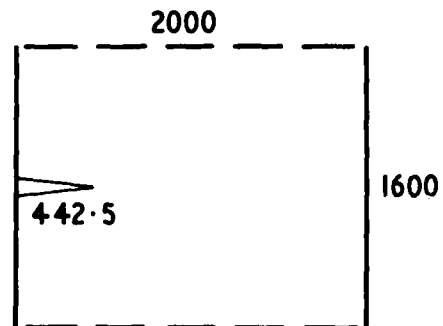
Roof & Floor : slotted 12% open

Side walls : solid

Fig 1   Tunnel working sections with NORA model (dimensions in mm).
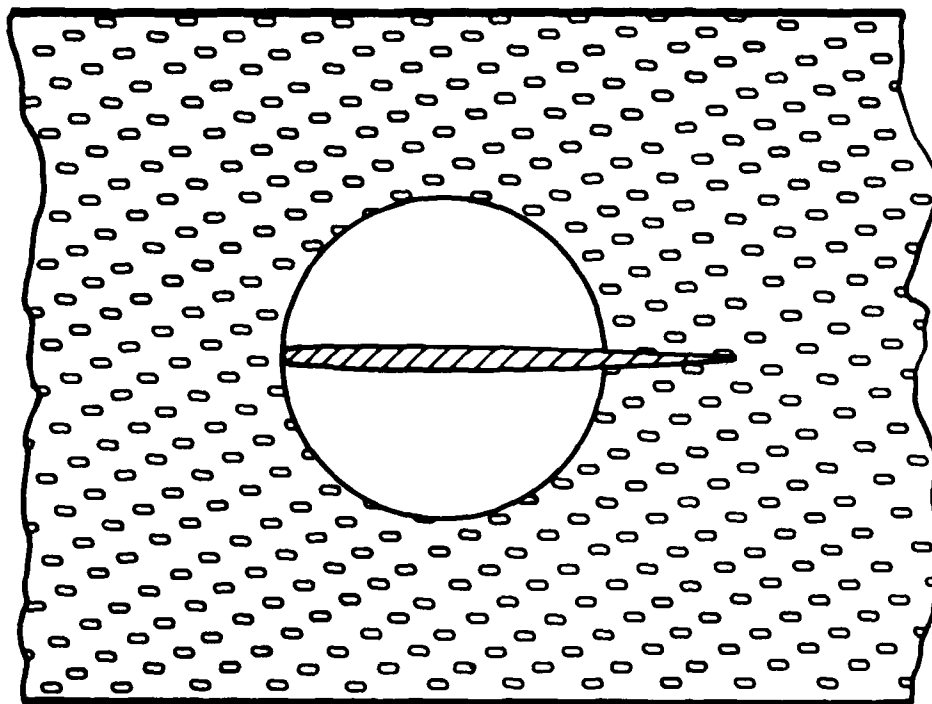
Fig 2   Mounting arrangement in 1M tunnel showing root chord of model in relation to the perforated wall.

Section	Position	Pressures
0	0·133 s	Steady
1	0·389	Steady
2	0·524	Unsteady
3	0·612	Steady
4	0·712	Unsteady
5	0·786	Steady
6	0·895	Steady
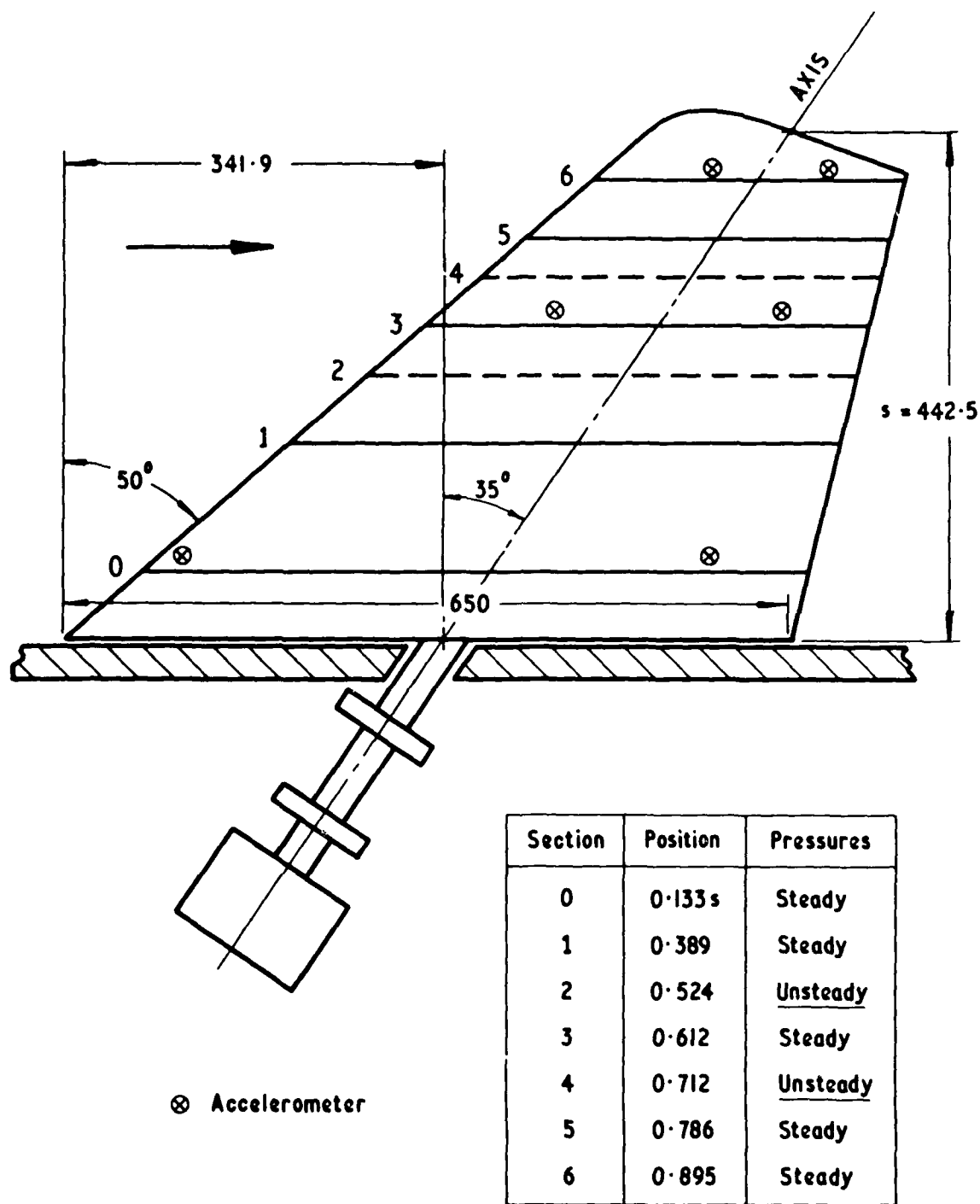
⊗ Accelerometer

Fig 3   NORA model and rotary oscillator (dimensions in mm).

Fig 4a   Model in 3Ft tunnel with rail at floor.

Fig 4b   Transportable measuring package.

60Hz

Design

Still-air

M = 0·9
∝ = 0
∝ = 4°

4

2

40Hz

Design and
Still-air

M = 0·9
∝ = 0
∝ = 4°

4

2
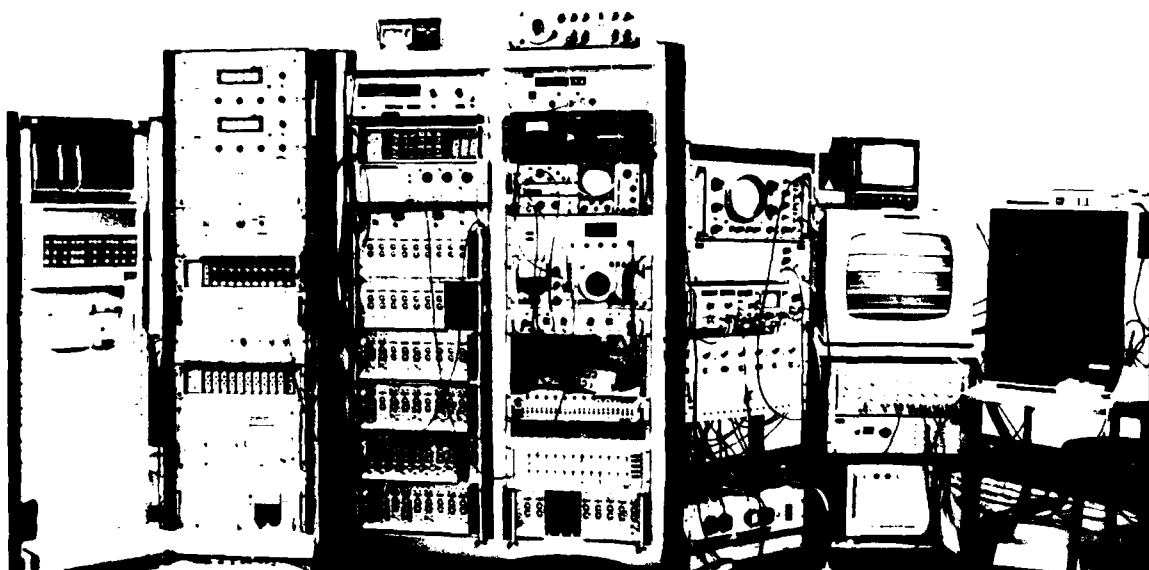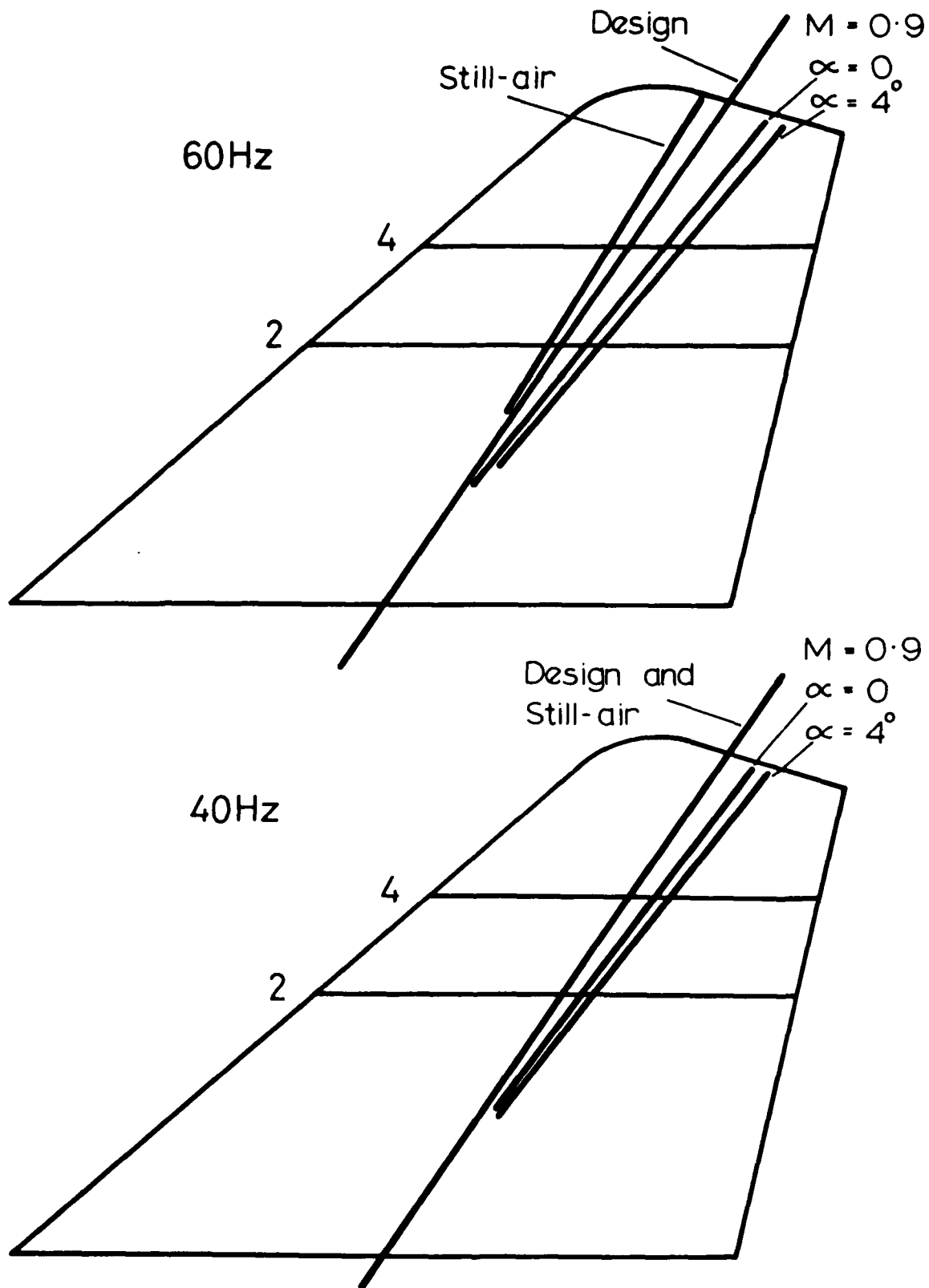
Fig 5   Position of oscillation axis as deduced from accelerometers.   Influence
of frequency and incidence.   (HST).

23
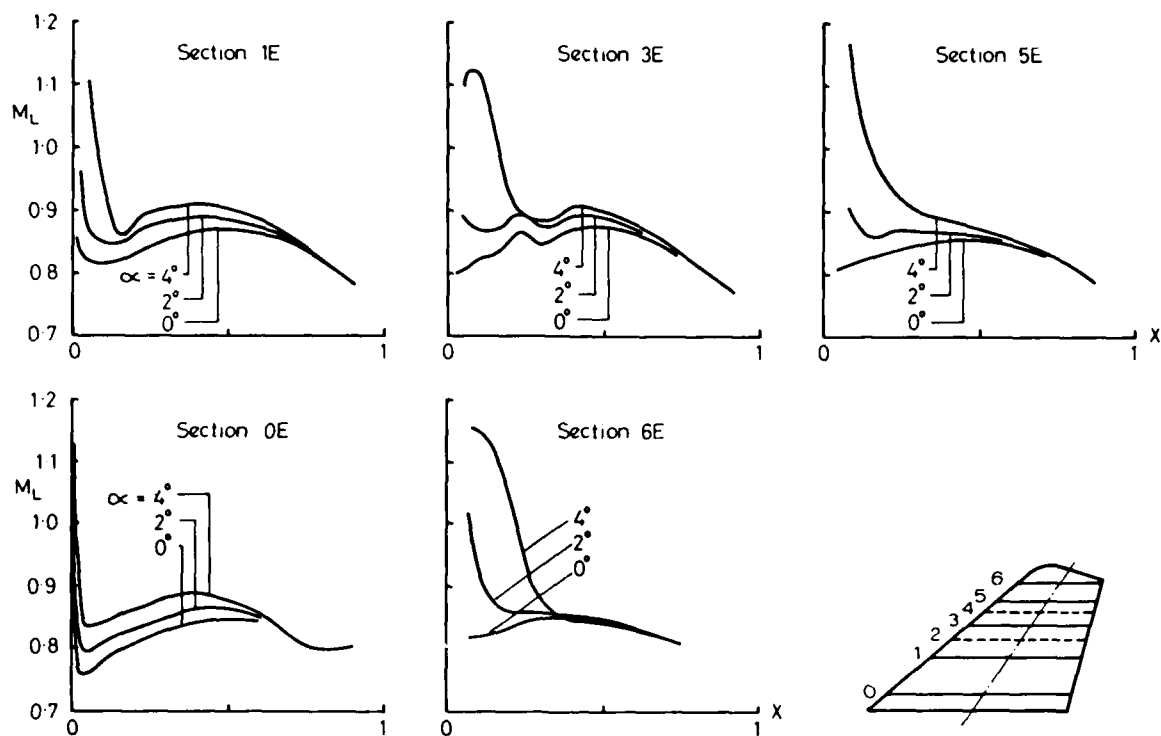
Fig 6   Local Mach numbers at upper surface, M = 0.80, in HST.
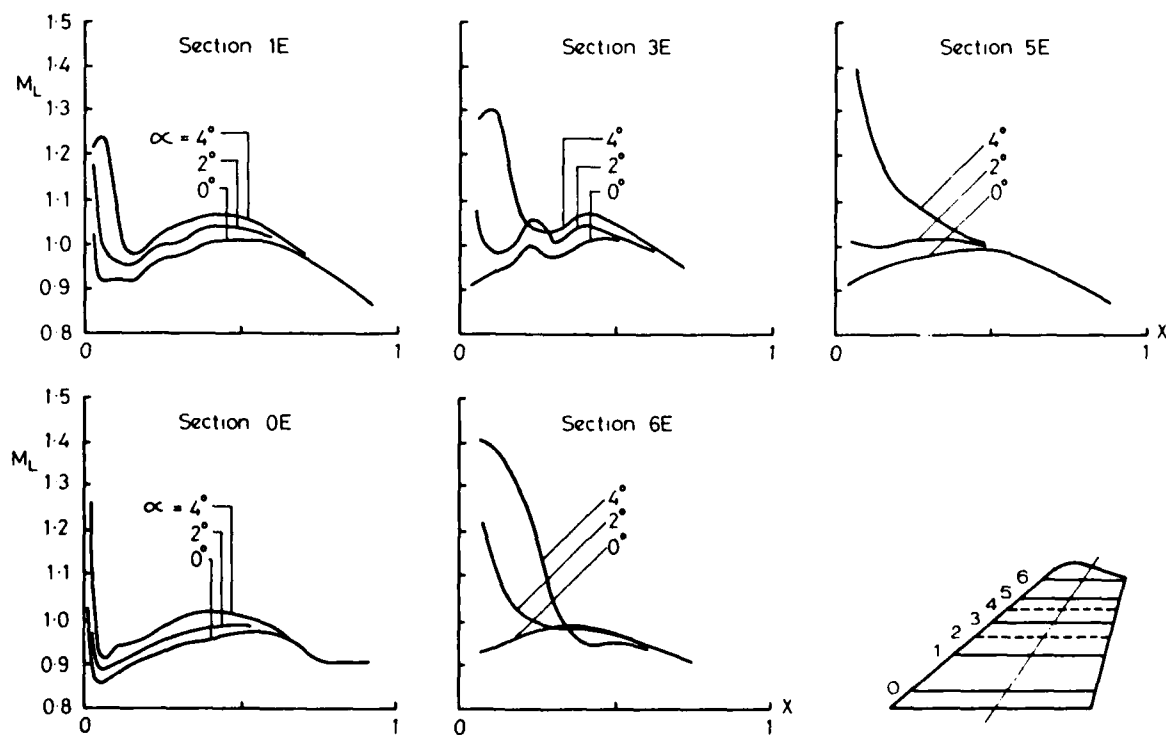
Fig 7   Local Mach numbers at upper surface, M = 0.90, in HST.

24
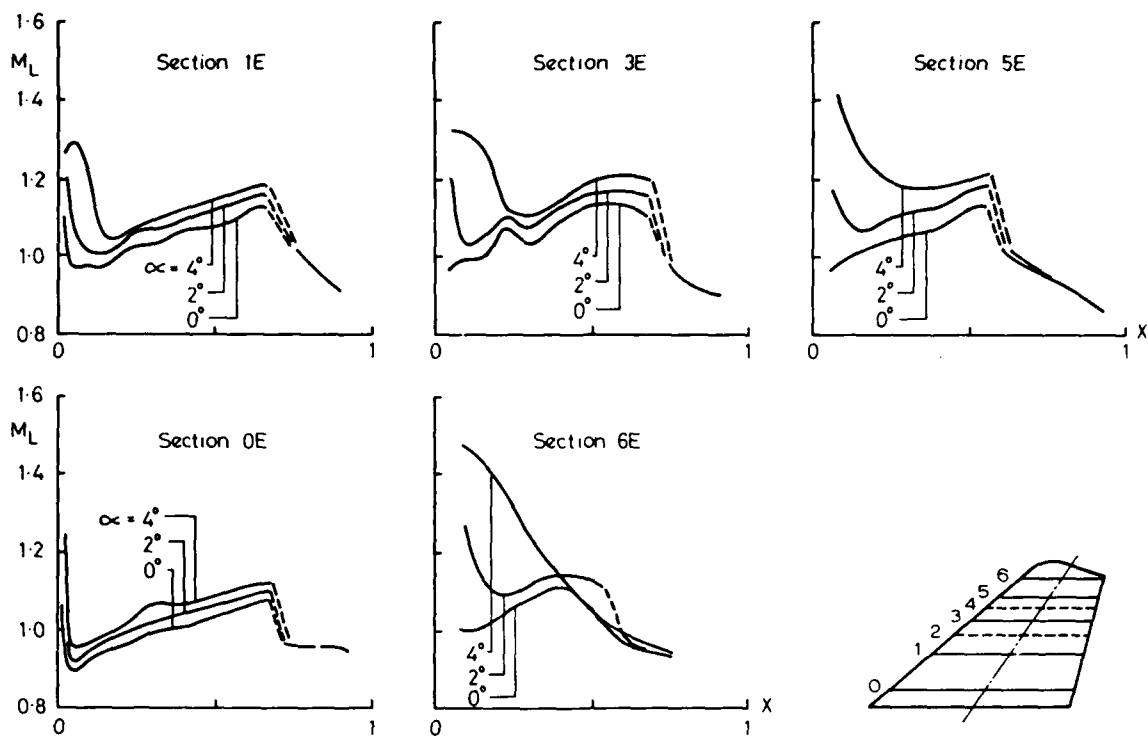
Fig 8   Local Mach numbers at upper surface, M = 0.95, in HST.
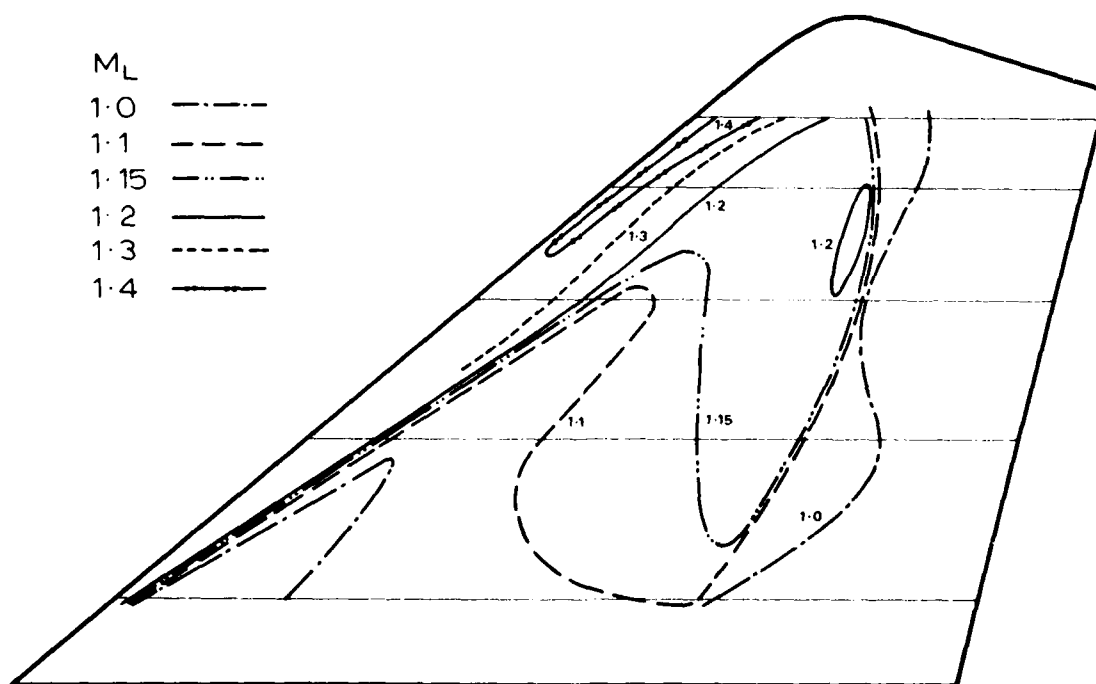
Fig 9   Iso-Mach lines, M = 0.95, α = 4°, in HST.
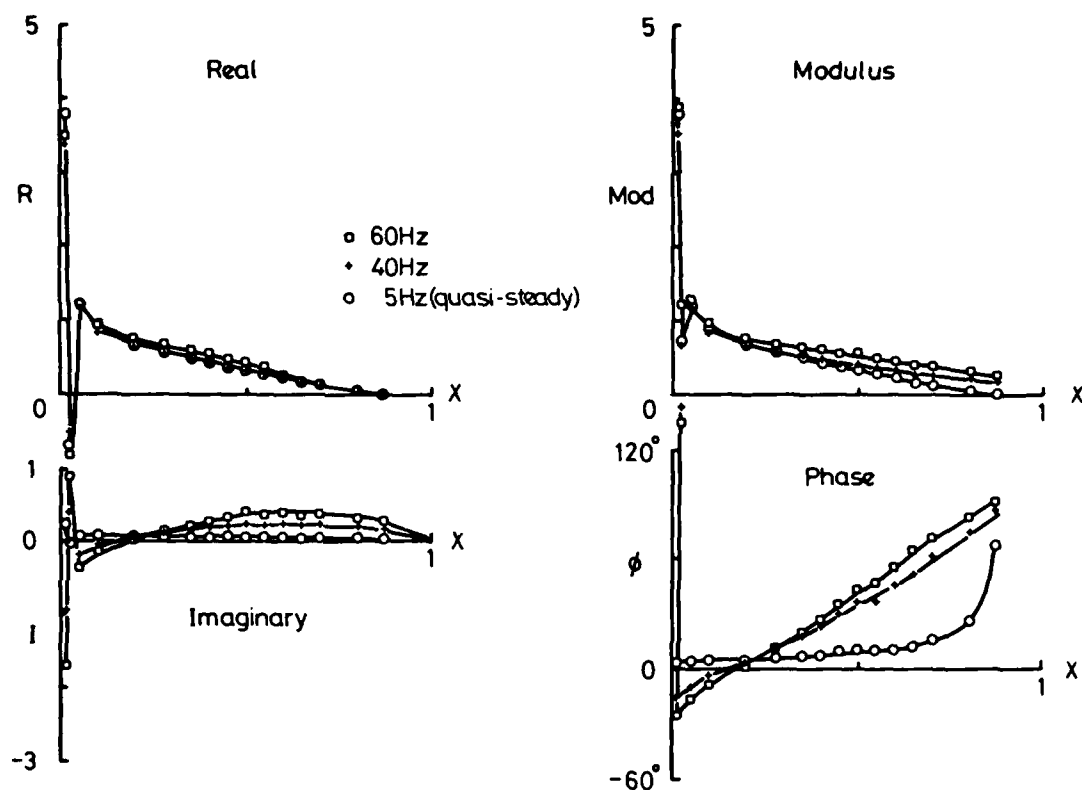
Fig 10   Oscillatory pressures, M = 0.80, α = 0. Influence of frequency,
Section 2E, HST.
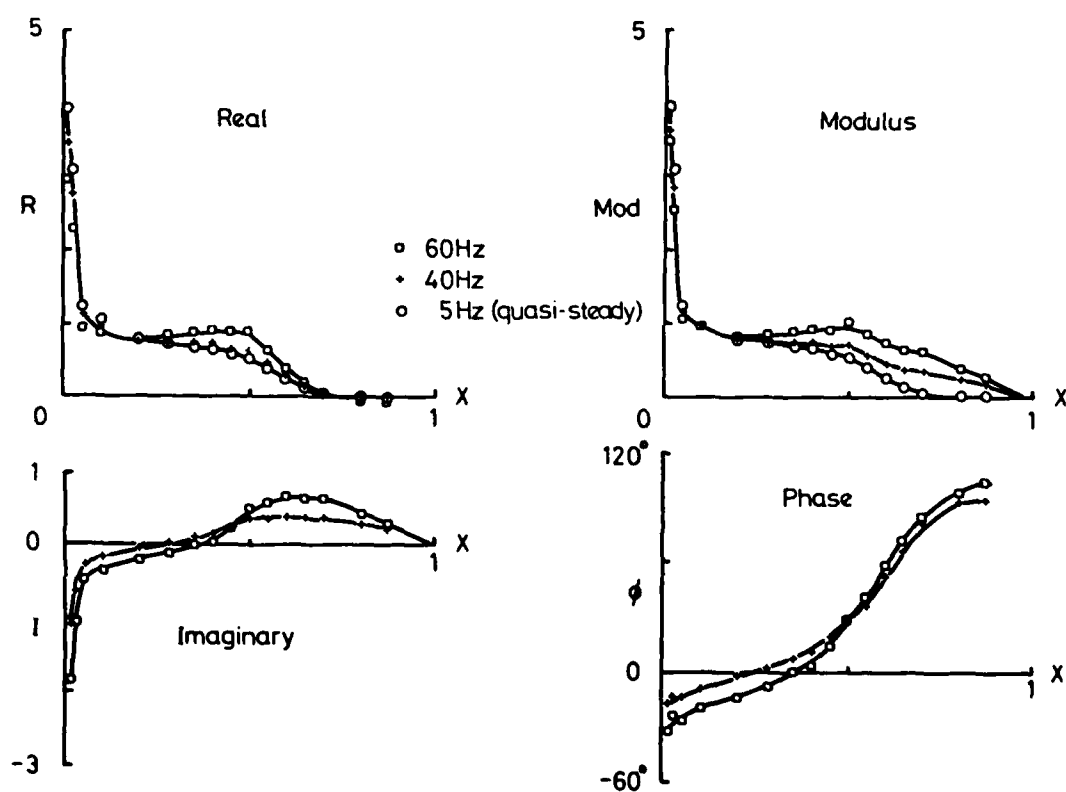
Fig 11   Oscillatory pressures, M = 0.90, α = 0. Influence of frequency,
Section 2E, HST.
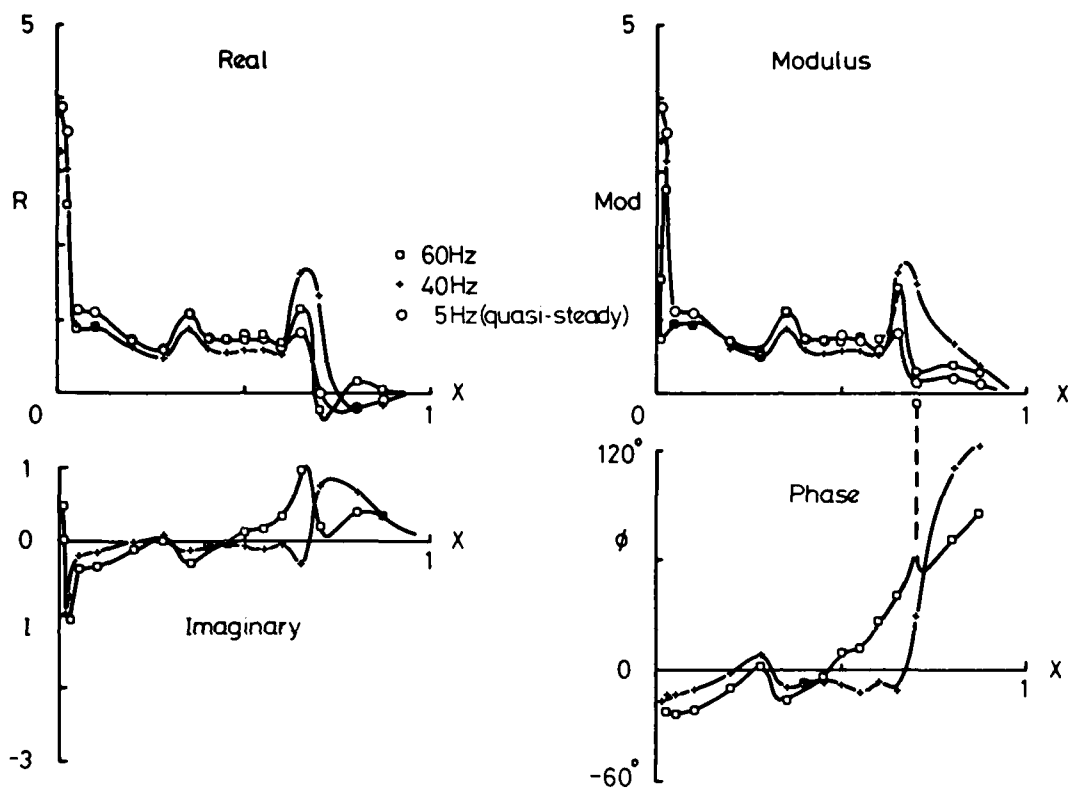
Fig 12   Oscillatory pressures, M = 0.95, α = 0. Influence of frequency,
          Section 2E, HST.
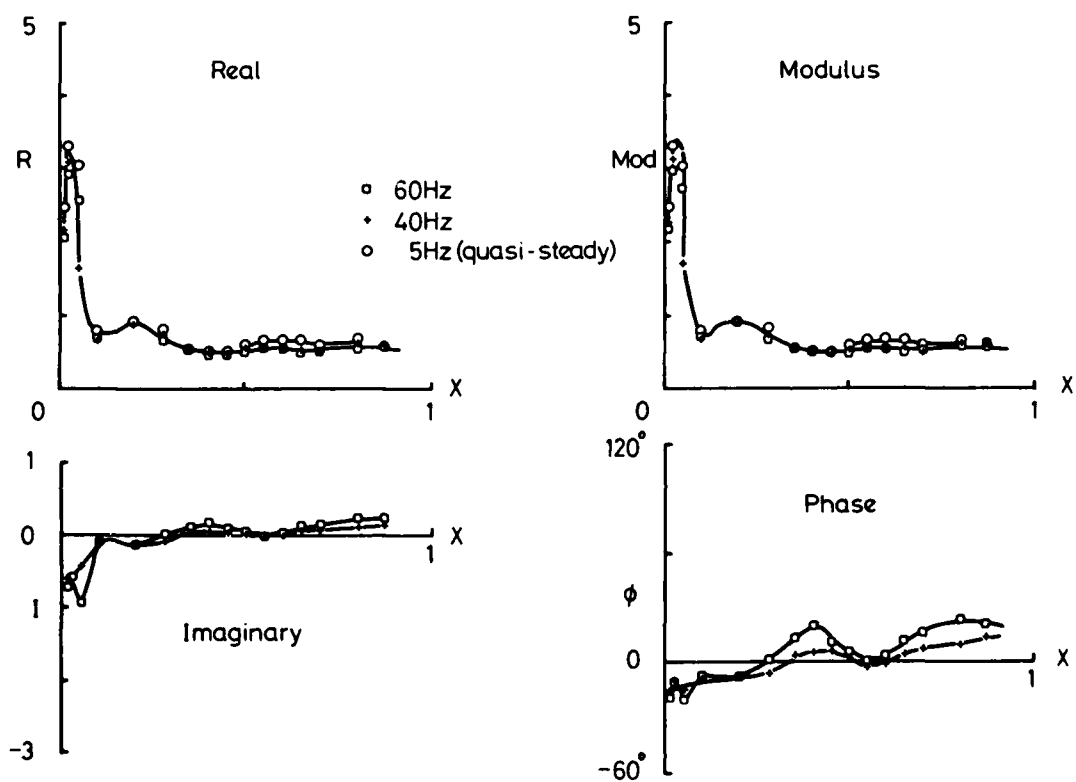
Fig 13   Oscillatory pressures, M = 1.10, α = 0. Influence of frequency,
          SEction 2E, HST.
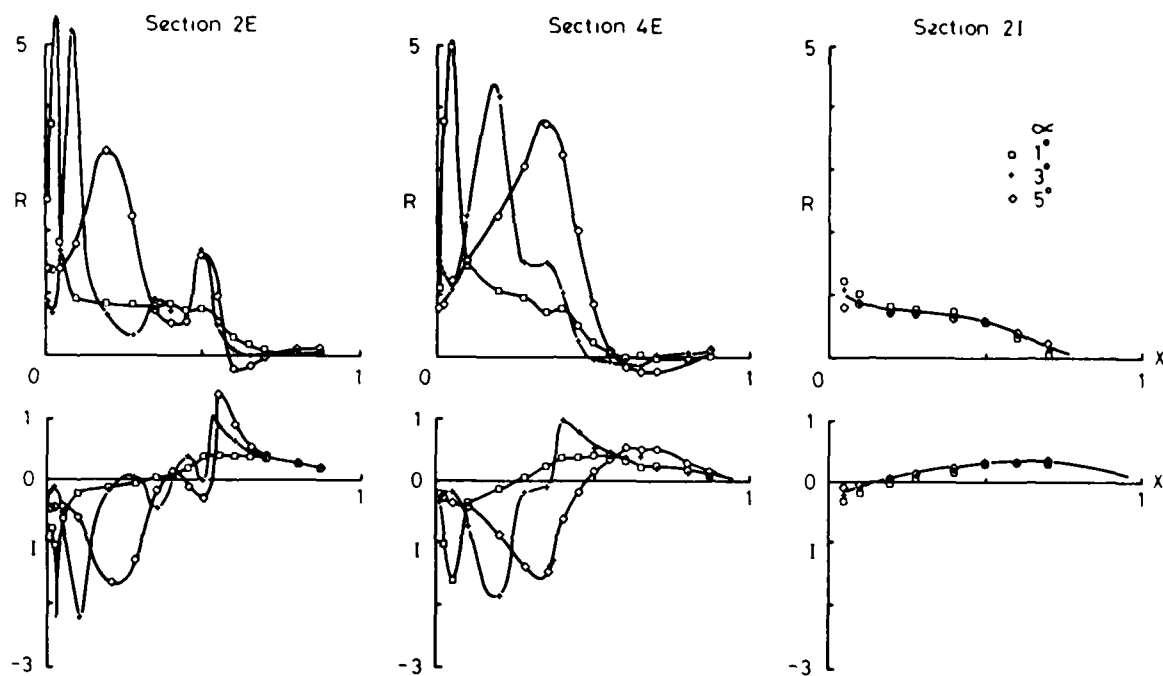
Fig 14 Oscillatory Pressures. Influence of incidence, M = 0.90, 40Hz, HST.
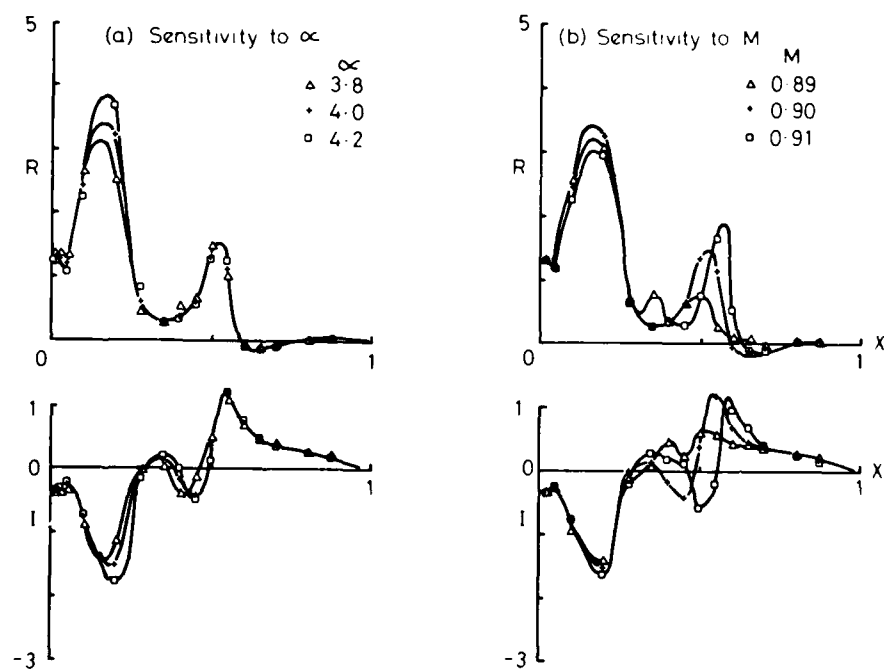
Fig 15 Oscillatory pressures. Sensitivity to small changes of incidence and Mach number. M = 0.90, α = 4°. Section 2E, 40Hz, HST.

28
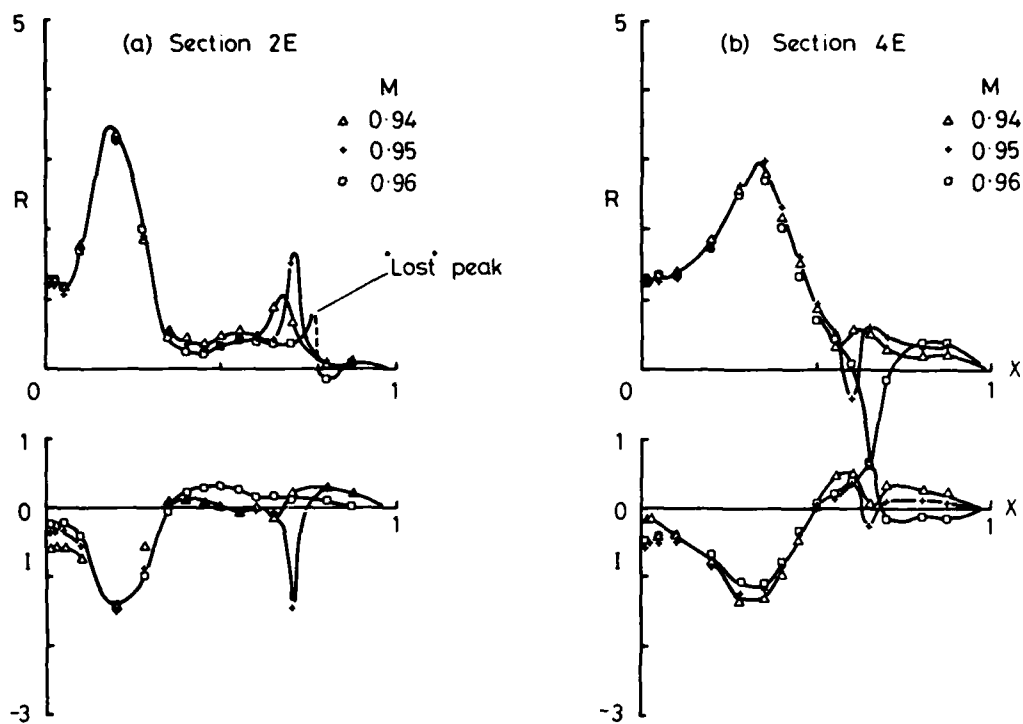
Fig 16   Oscillatory pressures. Sensitivity to small changes of Mach number.
M ≈ 0.95, α = 4.75°, f = 40Hz, HST.
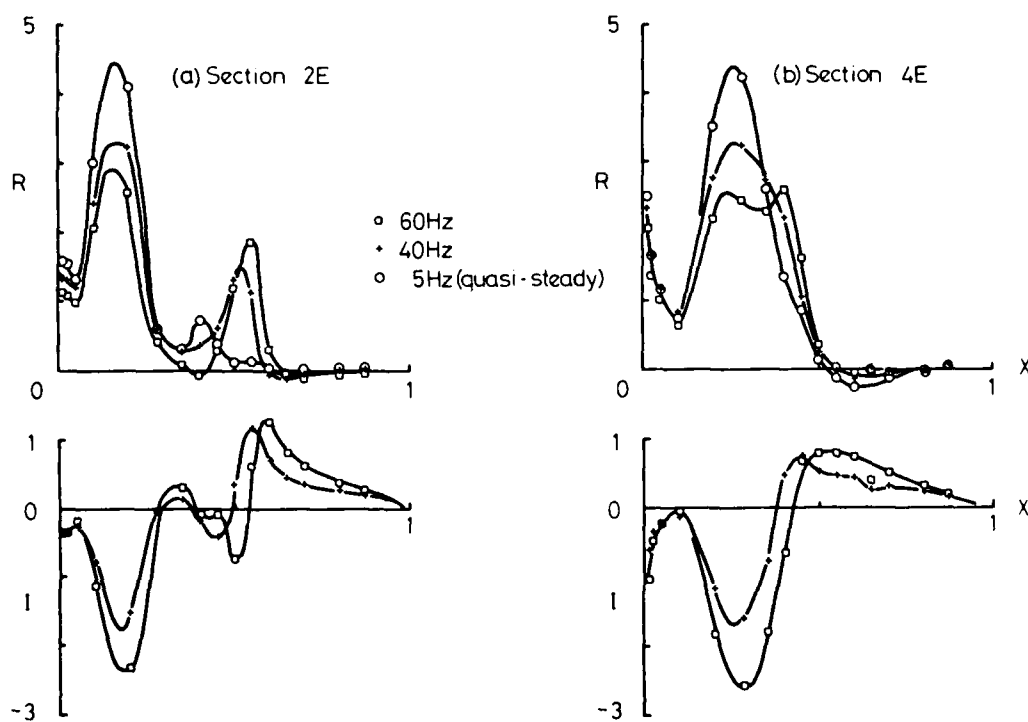
Fig 17   Oscillatory pressure. M ≈ 0.90, α = 4°. Influence of frequency, HST.
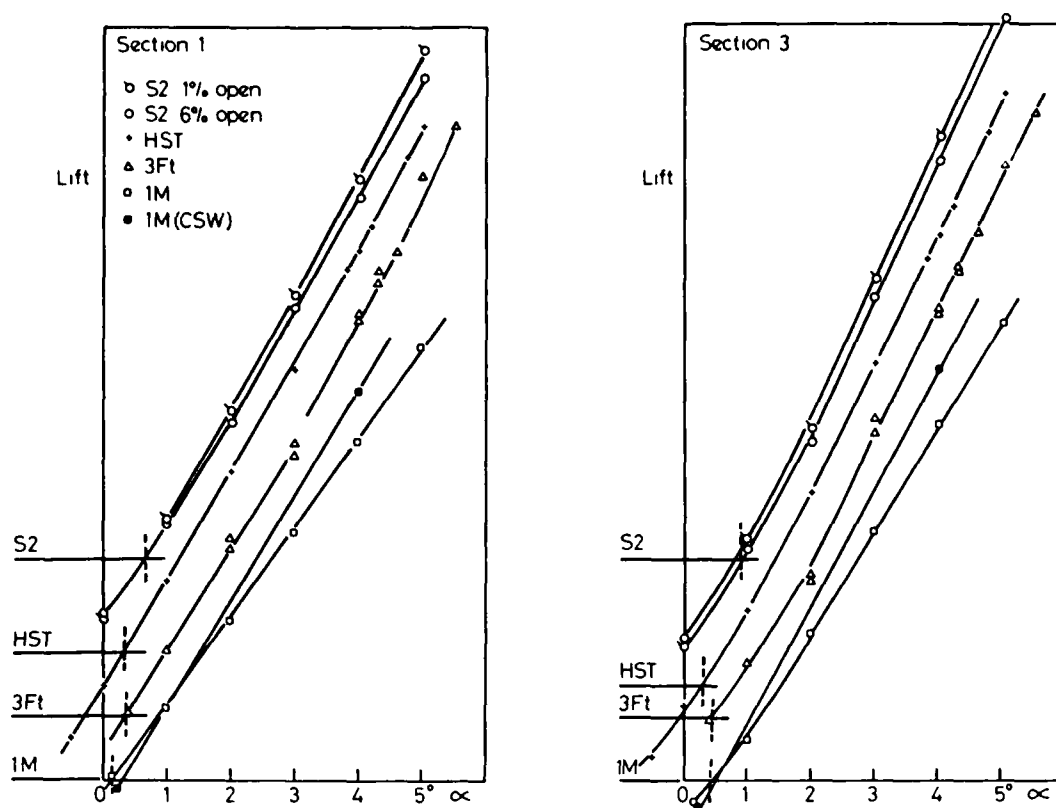
Fig 18   Variation of local lift with incidence, M = 0.90.
(Note: different lift origins for different tunnels).
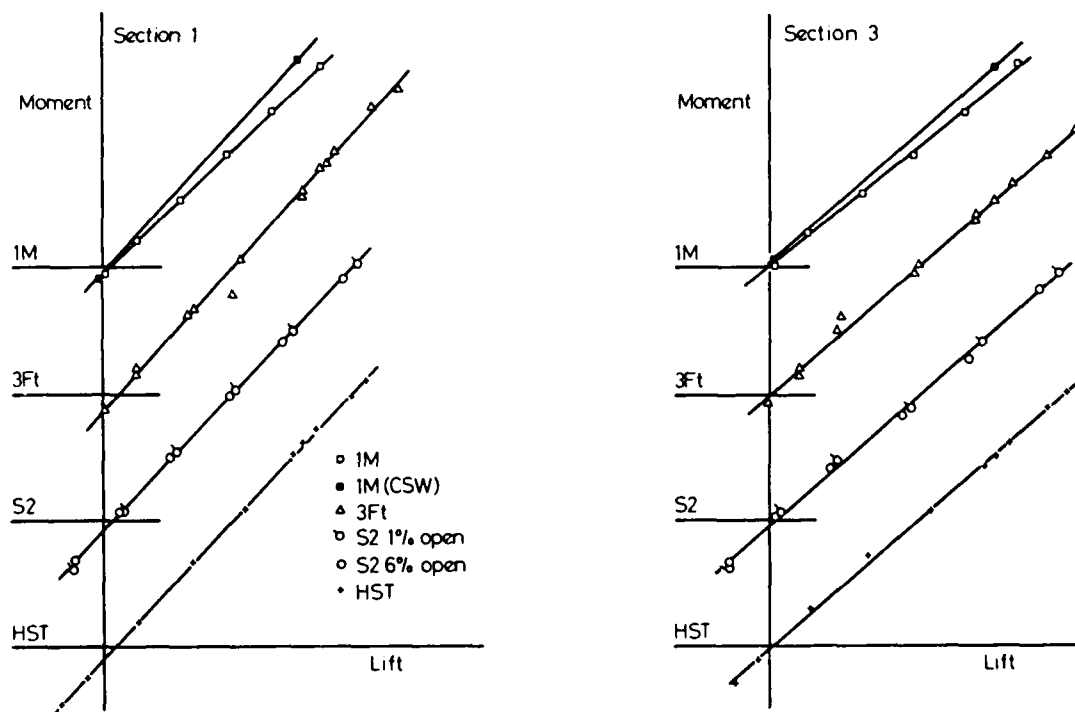
Fig 19   Variation of local pitching moment with lift, M = 0.90.
(Note: different moment origins for different tunnels).
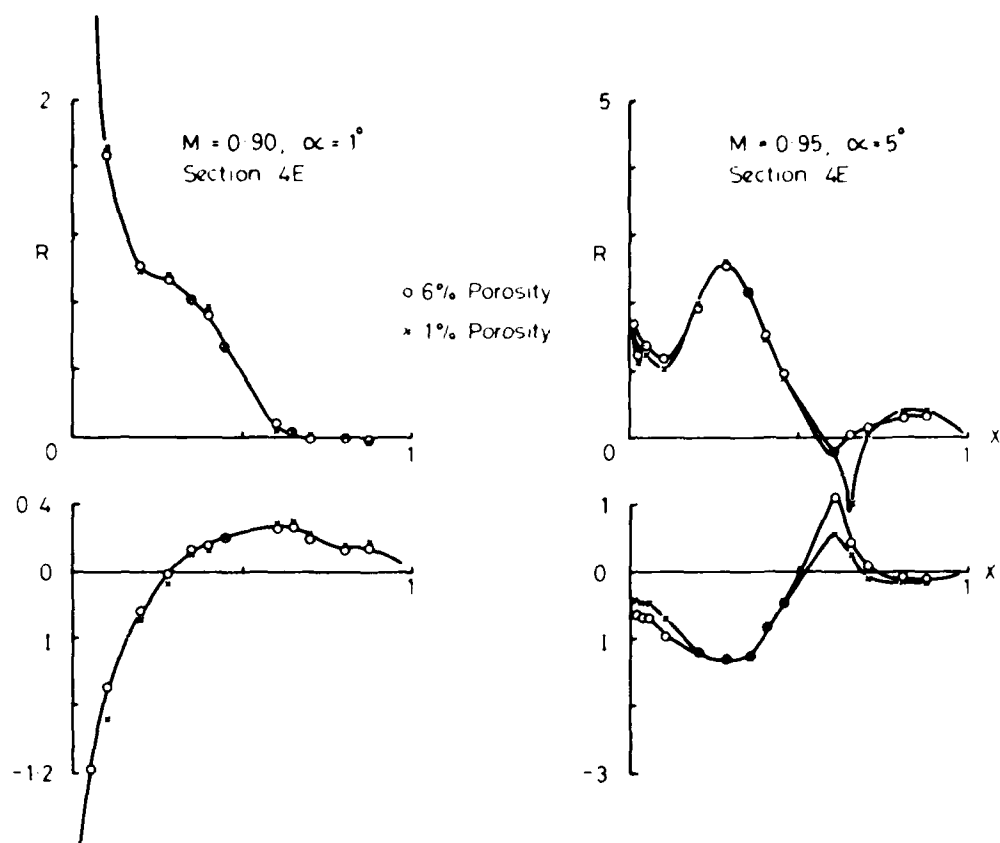
Fig 20   Oscillatory pressures.   Influence of porosity in S2, 40Hz, Section 4E.
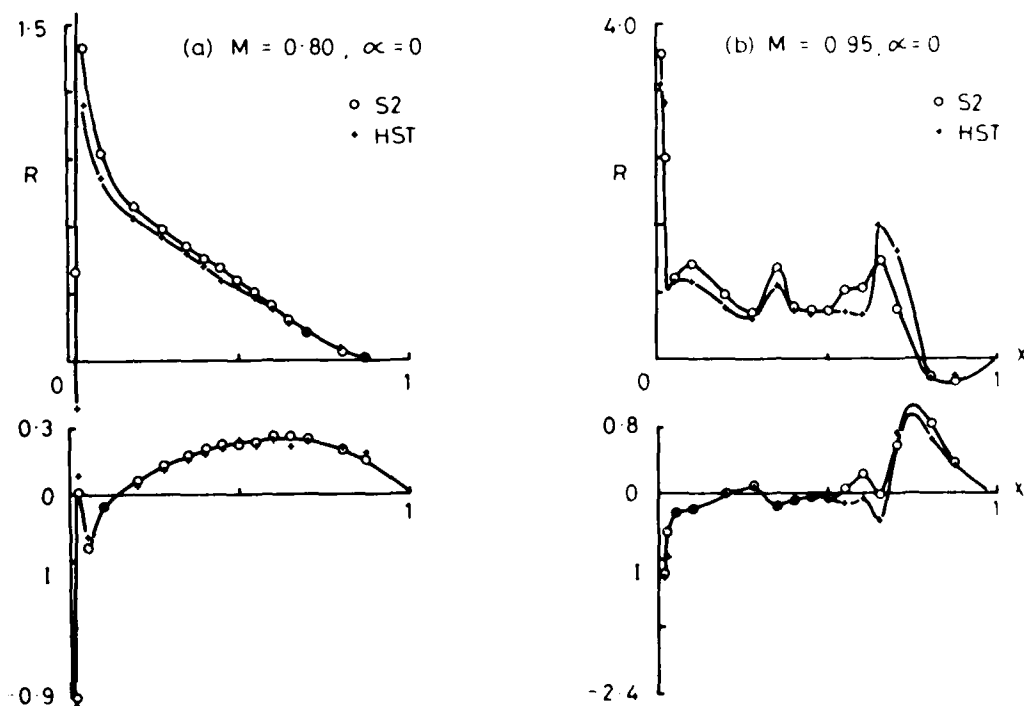
Fig 21   Oscillatory pressures.   Comparison of S2 and HST, Section 2E, 40Hz.
(a) M = 0.80, α = 0 and (b) M = 0.95, α = 0.
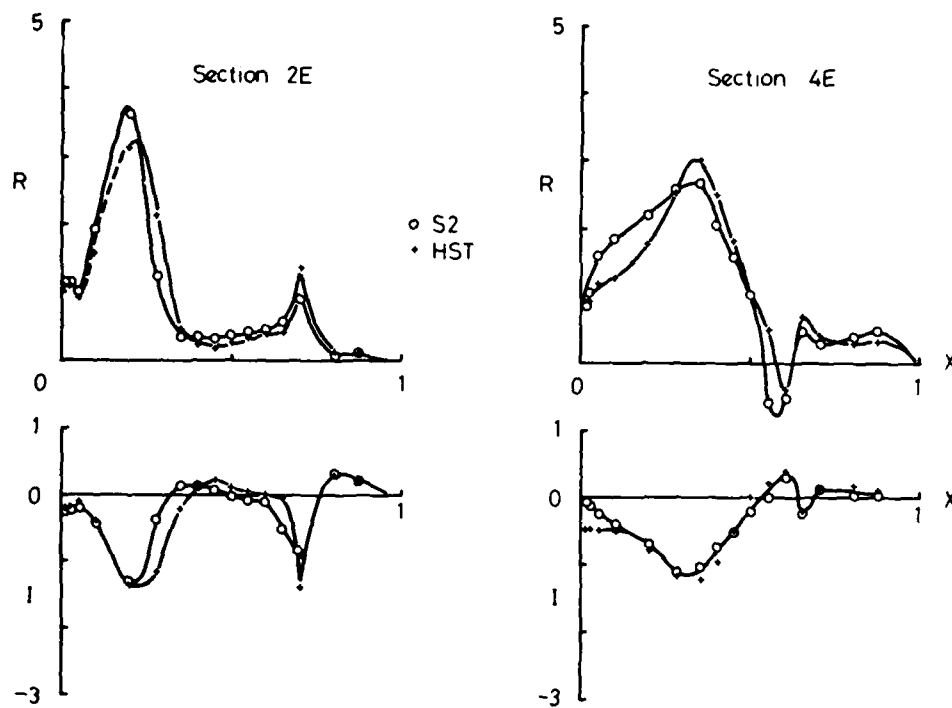
Fig 22   Oscillatory pressures. Comparison of S2 and HST.
M = 0.95, α = 5°, f = 40Hz.
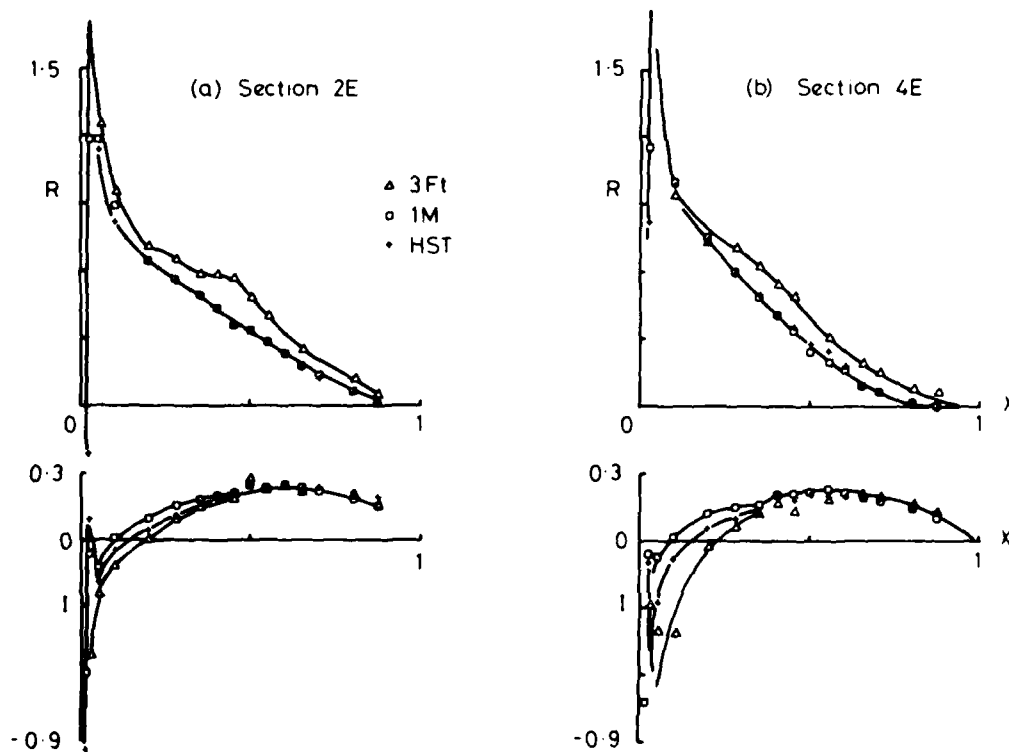
Fig 23   Oscillatory pressures. Comparison of 3Ft, 1M and HST. M = 0.80
α = 0, f = 40Hz.
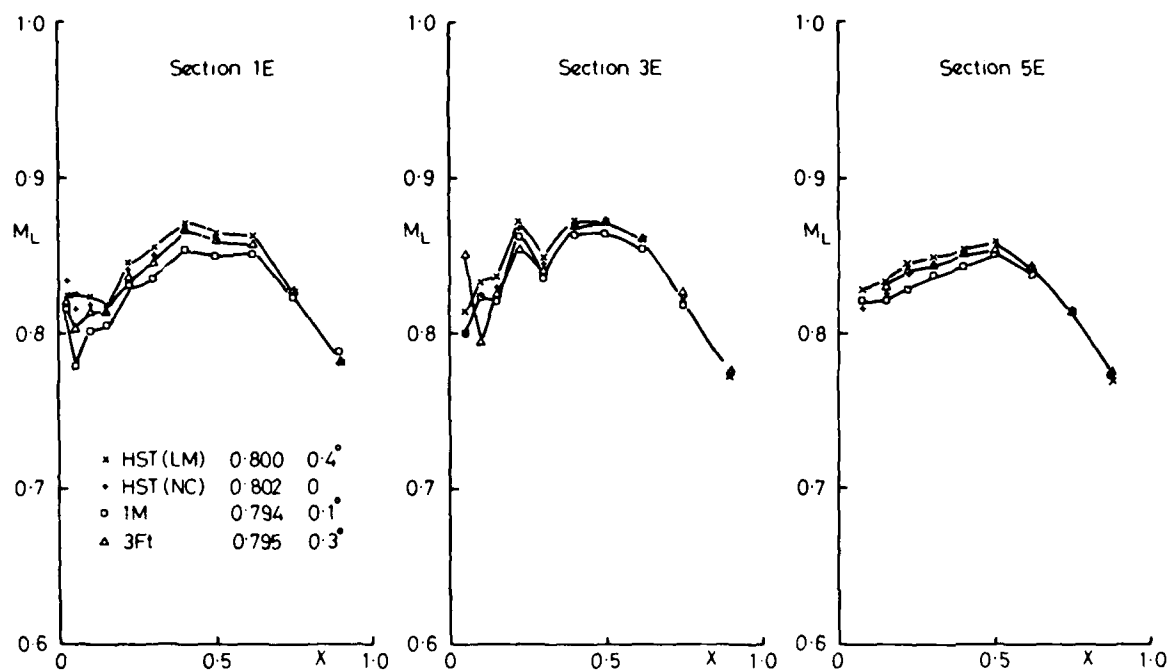
Fig 24   Local Mach numbers at upper surface. Comparison of 3Ft, 1M and HST.
M = 0.80 α = 0.

Fig 25   Oscillatory pressures. Comparison of 3Ft, 1M and HST. M = 0.90,
α = 0, f = 40Hz.

(a) HST

(b) 1M
□ 60Hz
• 40Hz
○ 5Hz (quasi-steady)

(c) 3Ft
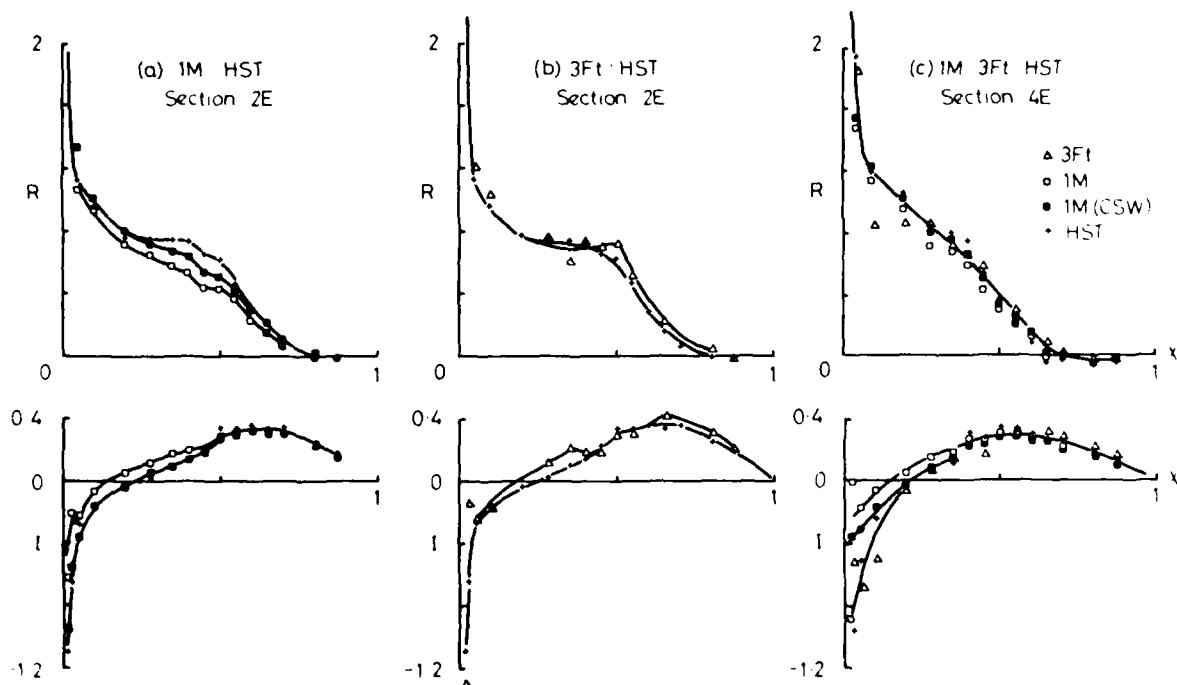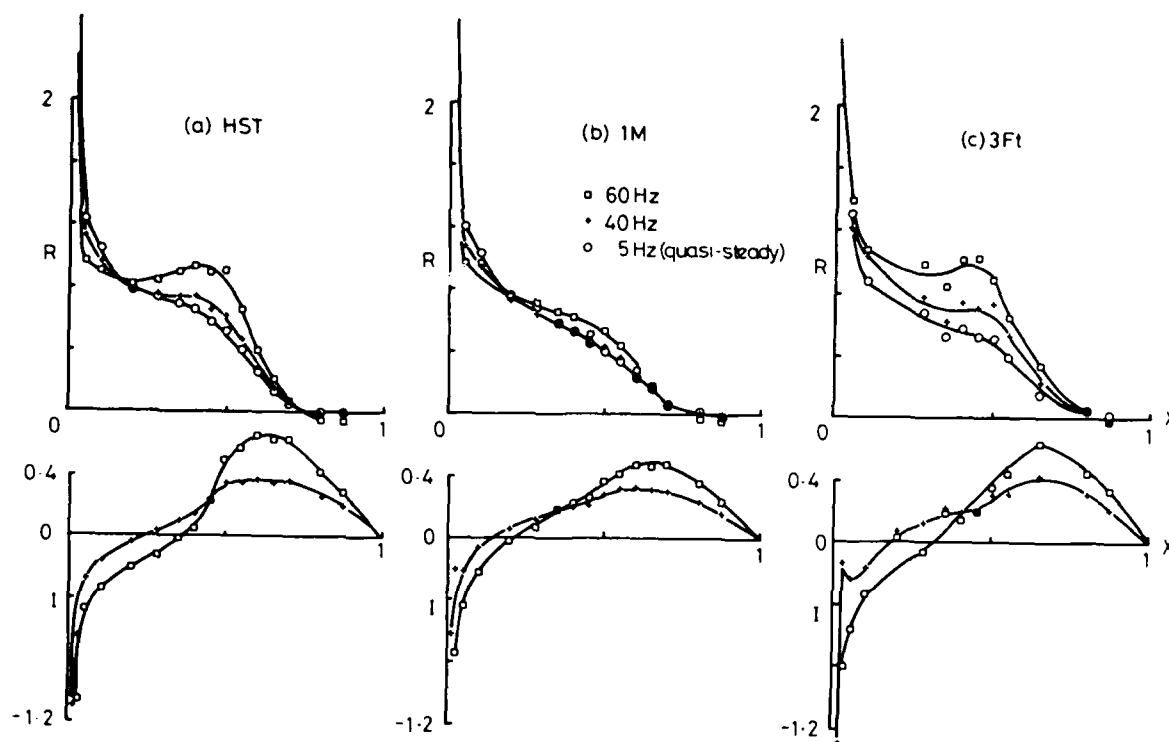
$\alpha \approx 0$, f = 40Hz.

Fig 26 Oscillatory pressures. Influence of frequency in different tunnels. M ≈ 0.90, $\alpha \approx 0$, Section 2E.

(a) 1M : HST

	M	$\propto$
• HST(NC)	0·954	0
× HST(PM)	0·941	0
○ 1M	0·945	0
△ 3Ft	0·945	0·6°

(b) 3Ft : HST
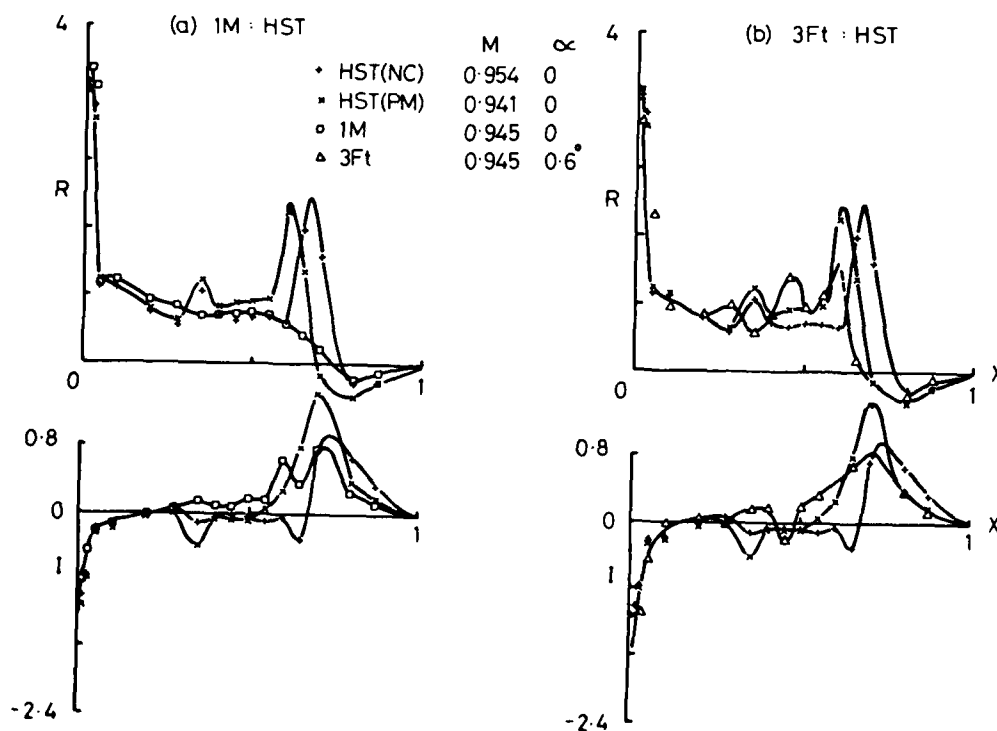
Fig 27 Oscillatory pressures. (a) Comparison of 1M and HST (b) Comparison of 3Ft and HST. M ≈ 0.95, $\alpha \approx 0$, Section 2E, 40Hz.
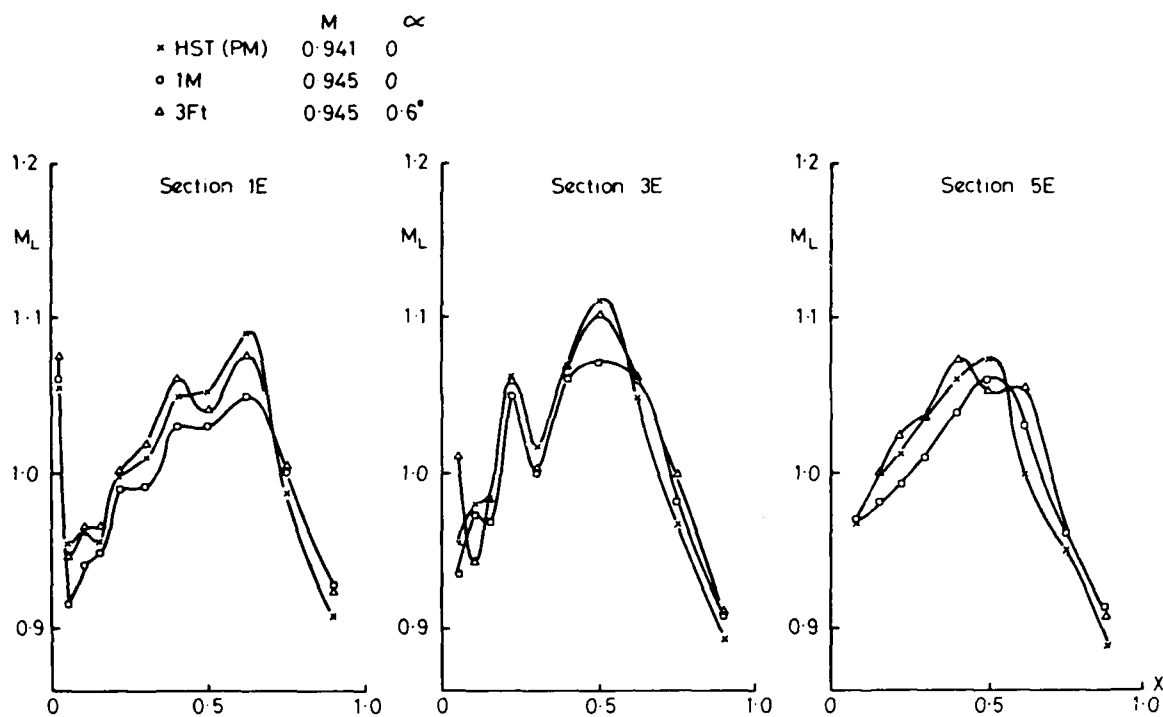
	M	α
× HST (PM)	0·941	0
○ 1M	0·945	0
△ 3Ft	0·945	0·6°

Section 1E

Section 3E

Section 5E

Fig 28   Local Mach numbers at upper surface.   Comparison of 3Ft, 1M and HST.
M ≈ 0.95, α ≈ 0.

(a) 1M : HST

□ 1M
✦ HST (LM)

(b) 3Ft : HST

△ 3Ft
✦ HST (LM)
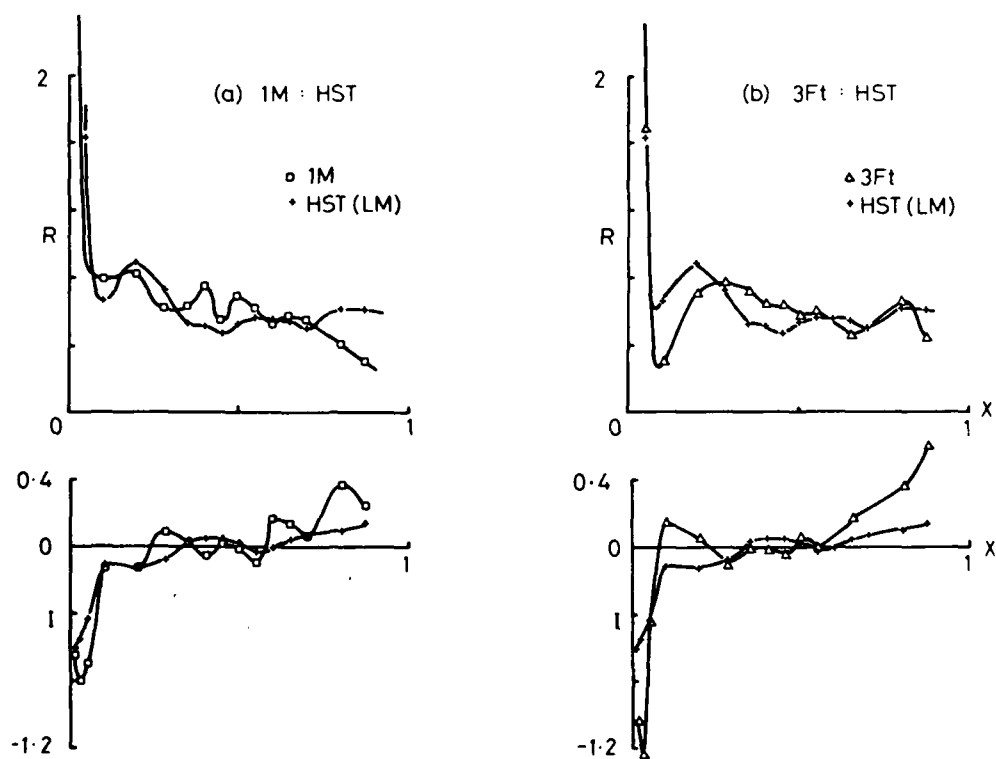
Fig 29   Oscillatory pressures.   (a) Comparison of 1M and HST (b) Comparison
of 3Ft and HST.   M ≈ 1.10, α ≈ 0 Section 2E, 40Hz.
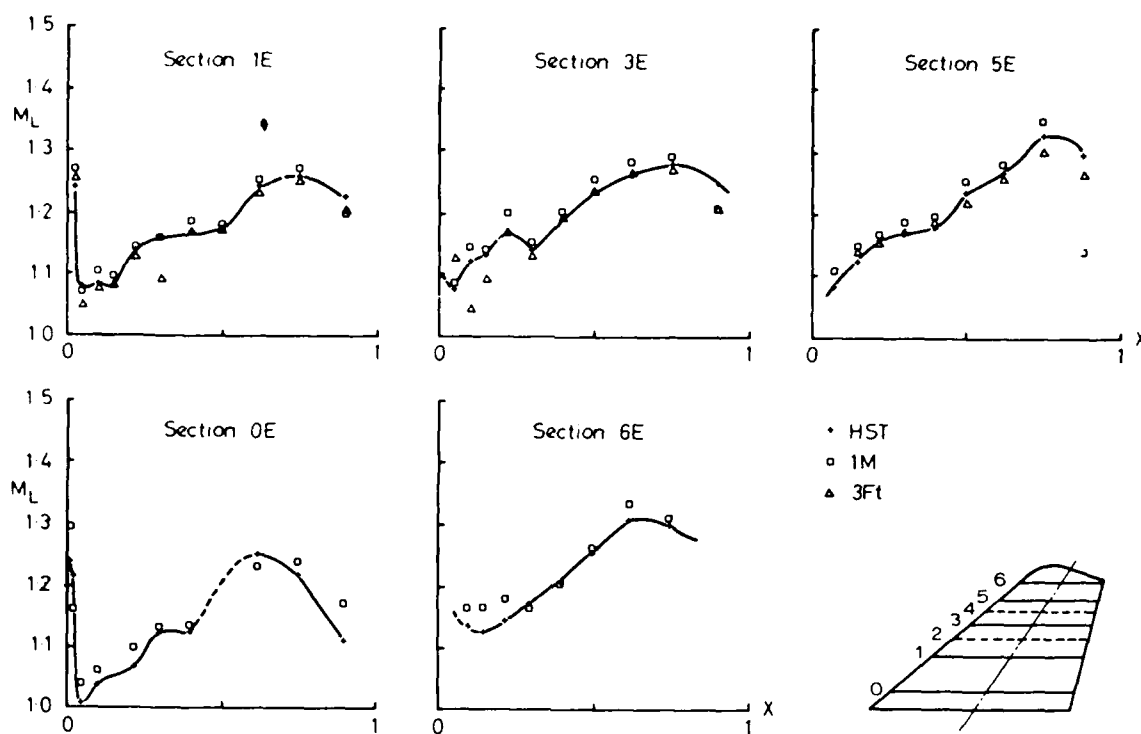
Fig 30   Local Mach numbers at upper surface. Comparison of 3Ft, 1M and HST.
M ≈ 1.10 α ≈ 0.
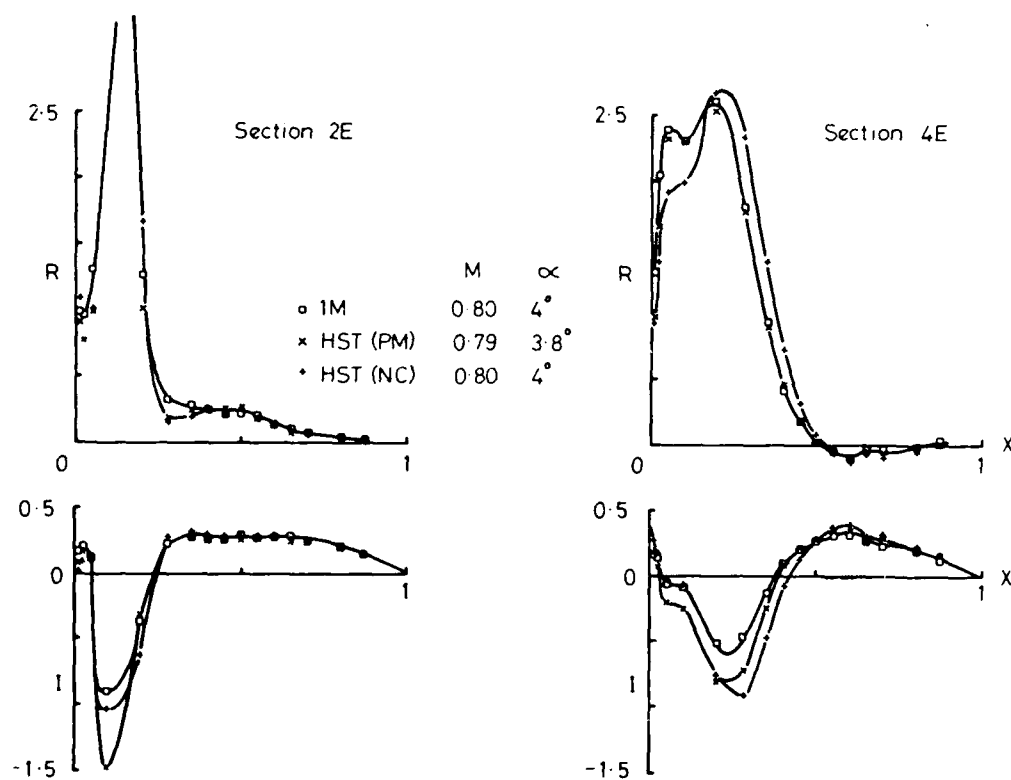
Fig 31   Oscillatory pressures. Comparison of 1M and HST. M ≈ 0.80,
α ≈ 4°, f = 40Hz.
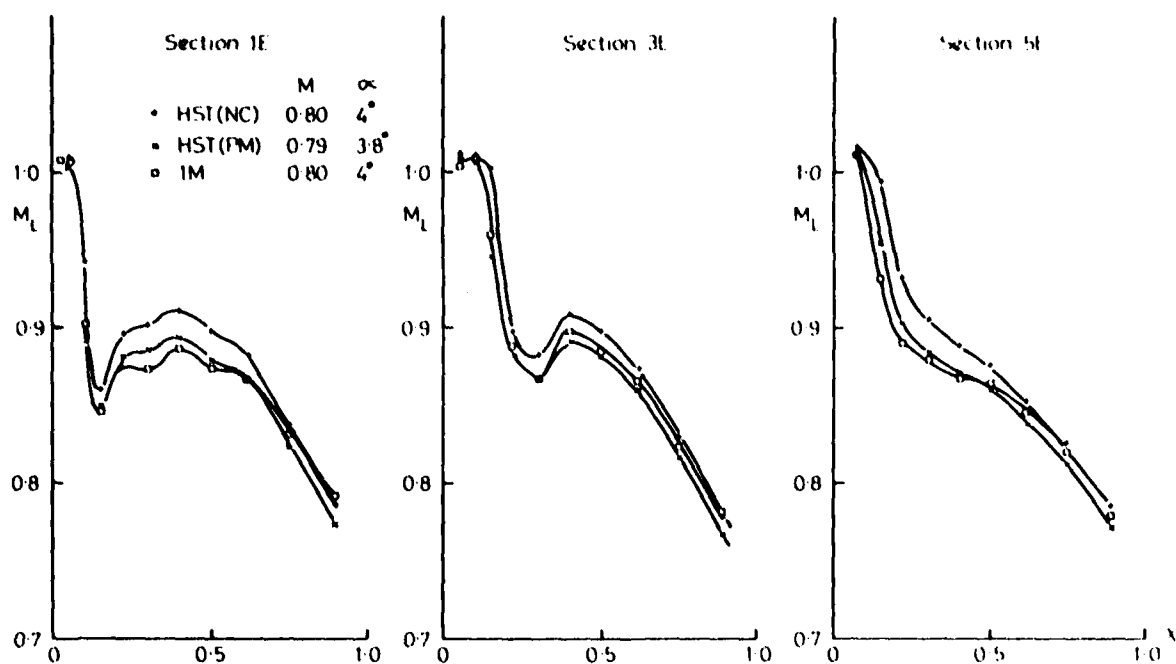
Fig 42   Local Mach number at upper surface. Comparison of 1M and HST.
M = 0.80, α = 4°.
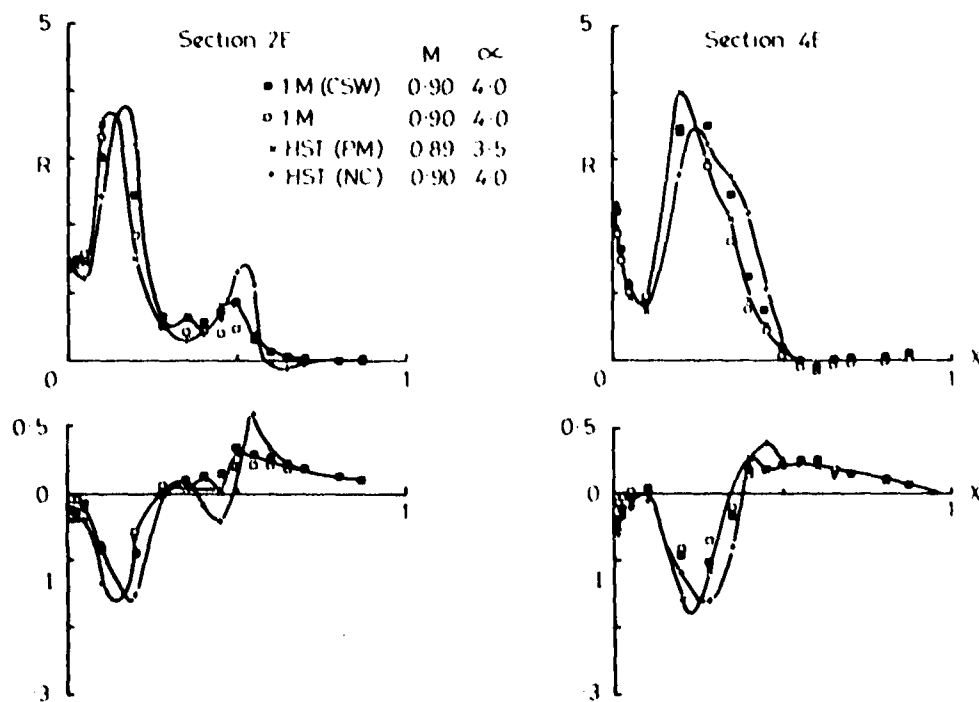
Fig 43   Oscillatory pressures. Comparison of 1M and HST. M = 0.90,
α = 4°, f = 60Hz.
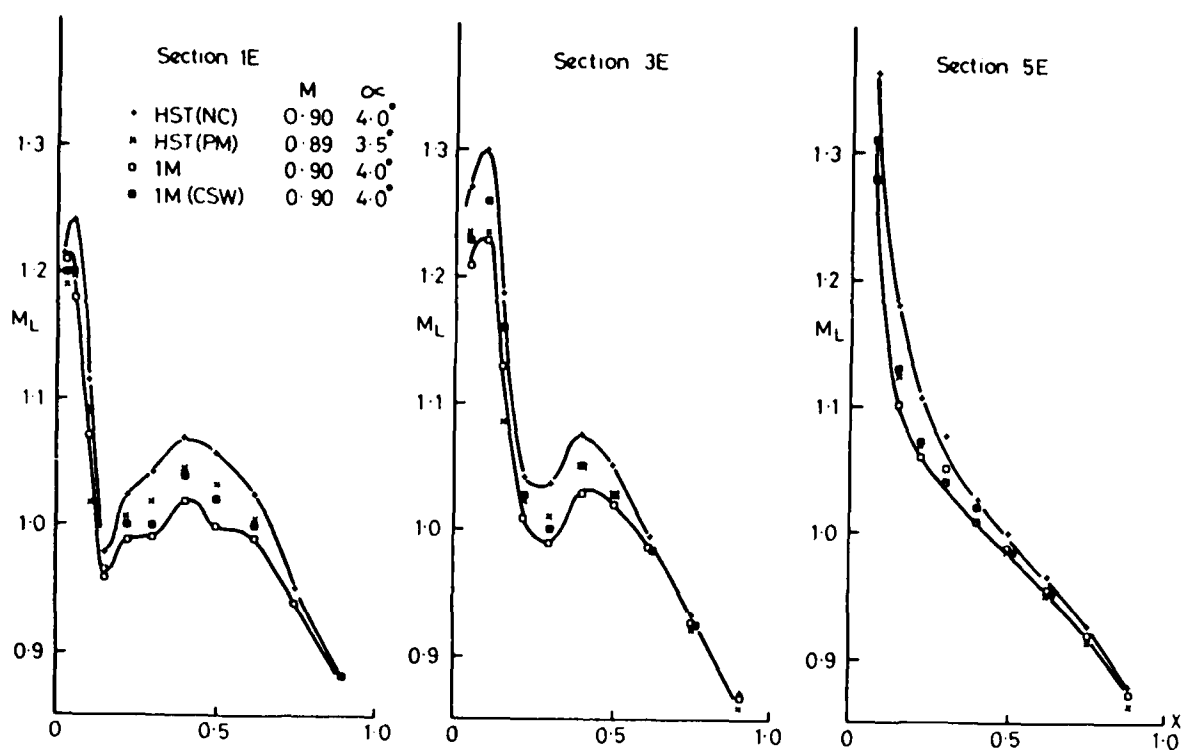
Fig 34   Local Mach numbers at upper surface.   Comparison of 1M and HST.
M = 0.90, α = 4°.
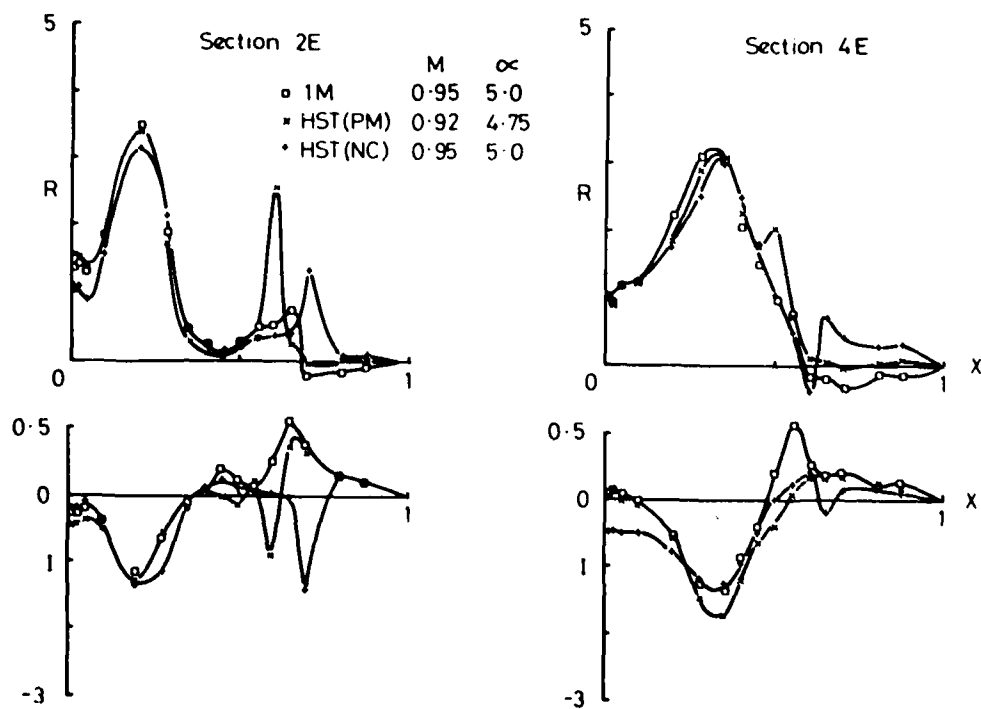
Fig 35   Oscillatory pressures.   Comparison of 1M and HST.   M = 0.95,
α = 5°, f = 40Hz.
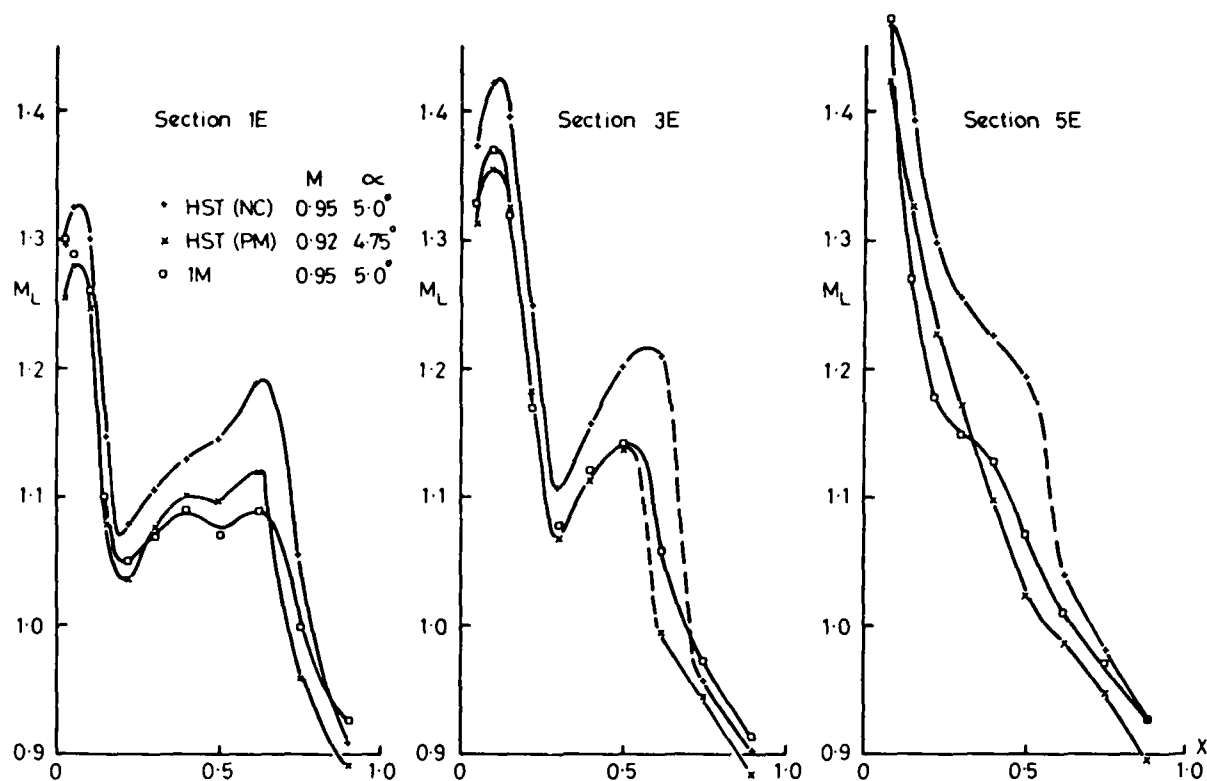
Fig 36   Local Mach numbers at upper surface.   Comparison of 1M and HST.
M ≈ 0.95, α ≈ 5°.
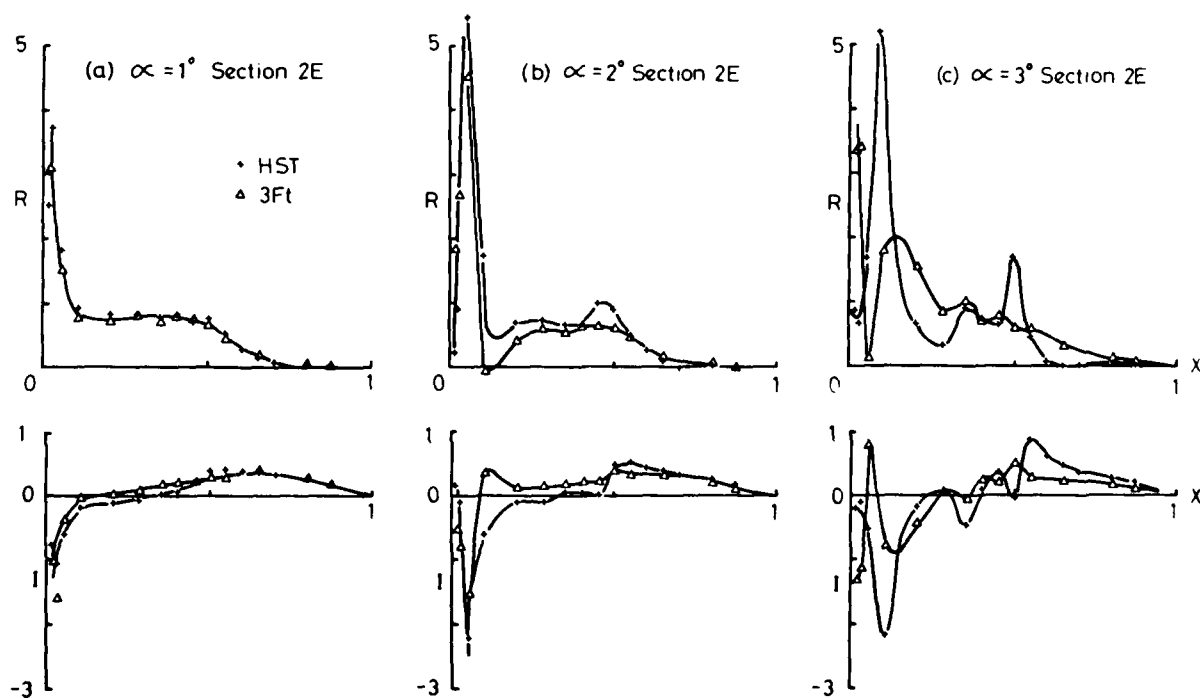
Fig 37   Oscillatory pressures.   Effects of increasing incidence in 3Ft and HST.
M = 0.90, f = 40Hz (continued in Fig 38).

39

(a) $\alpha = 4°$ Section 2E   (b) $\alpha = 5°$ Section 2E   (c) $\alpha = 4°$ Section 4E
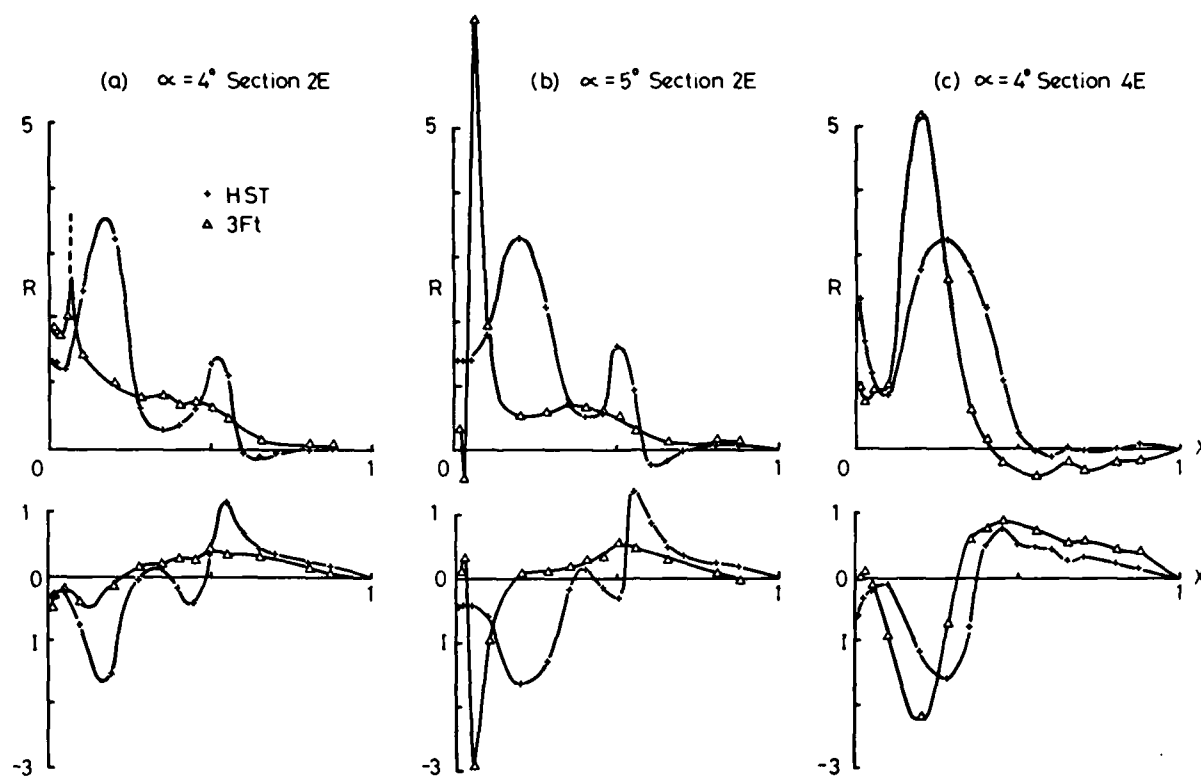
Fig 38   (Continued from Fig 37).
Oscillatory pressures. Effects of increasing incidence in 3Ft and HST.
M = 0.90, f = 40Hz.

Section 1E

	M	α
✦ HST(NC)	0·90	4·0°
× HST(PM)	0·89	3·5°
△ 3Ft	0·90	4·0°

Section 3E

Section 5E
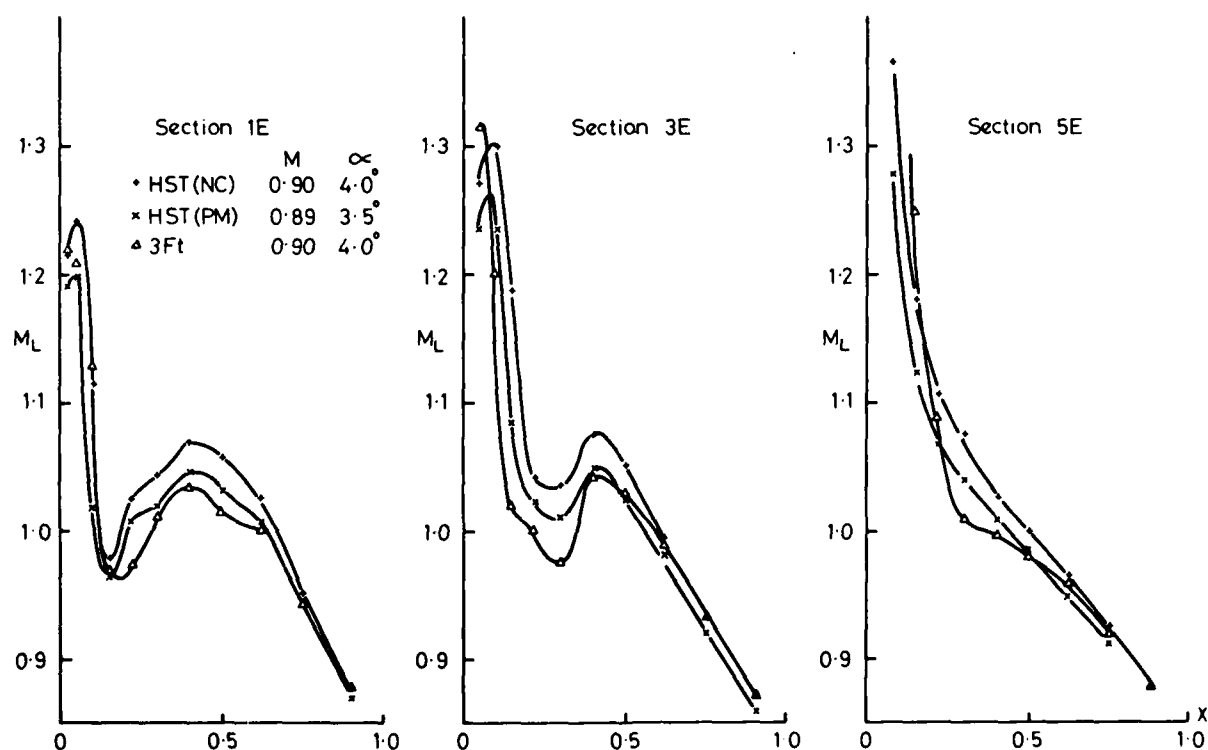
Fig 39   Local Mach numbers at upper surface. Comparison of 3Ft and HST.
M = 0.90 α ~ 4°.

40
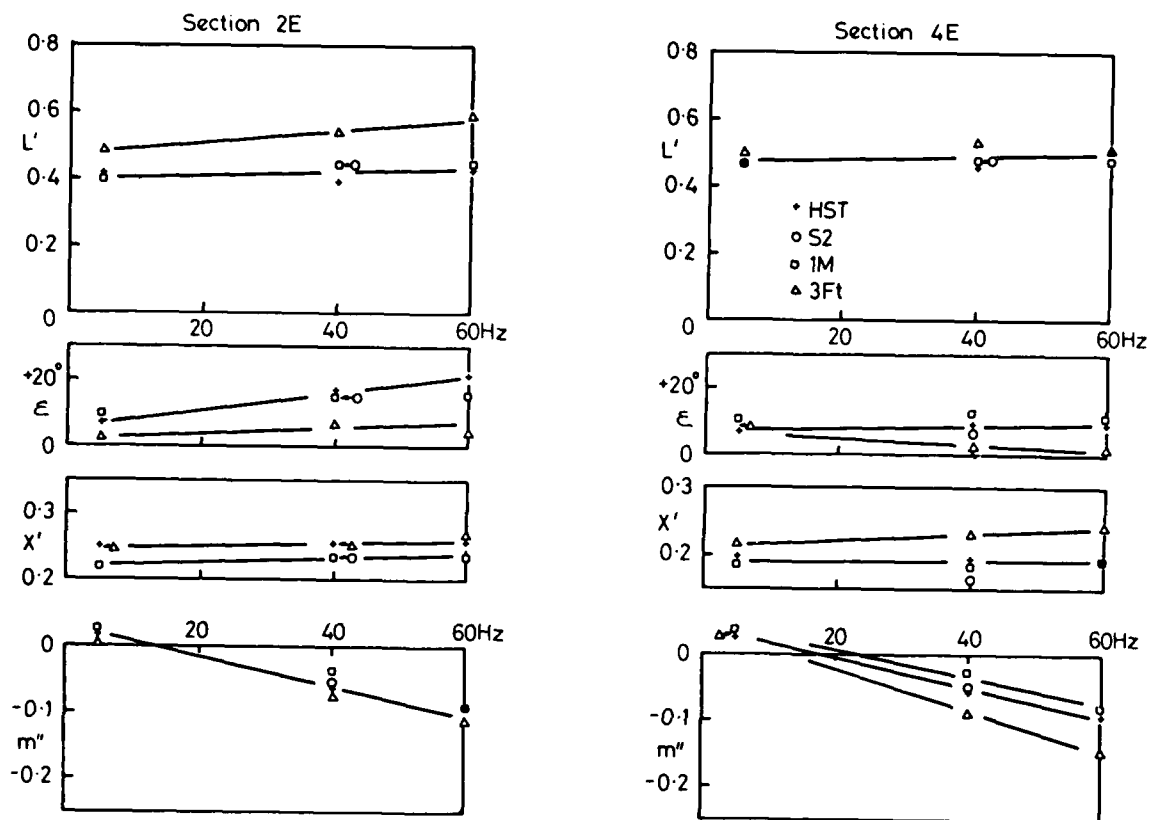
Fig 40   Variation of upper surface chordal properties with frequency.
M = 0.80, α = 0.

41
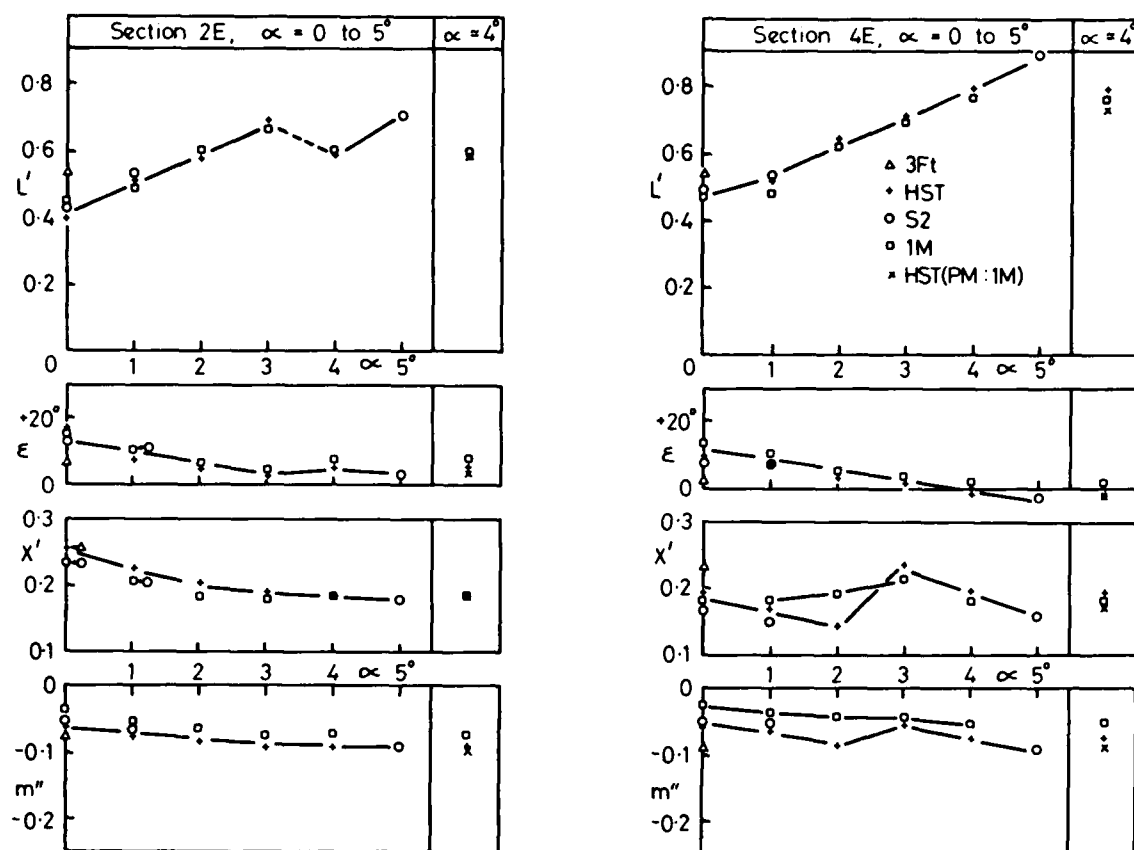
Fig 41   Variation of upper surface chordal properties with incidence.
M = 0.80, f = 40Hz.
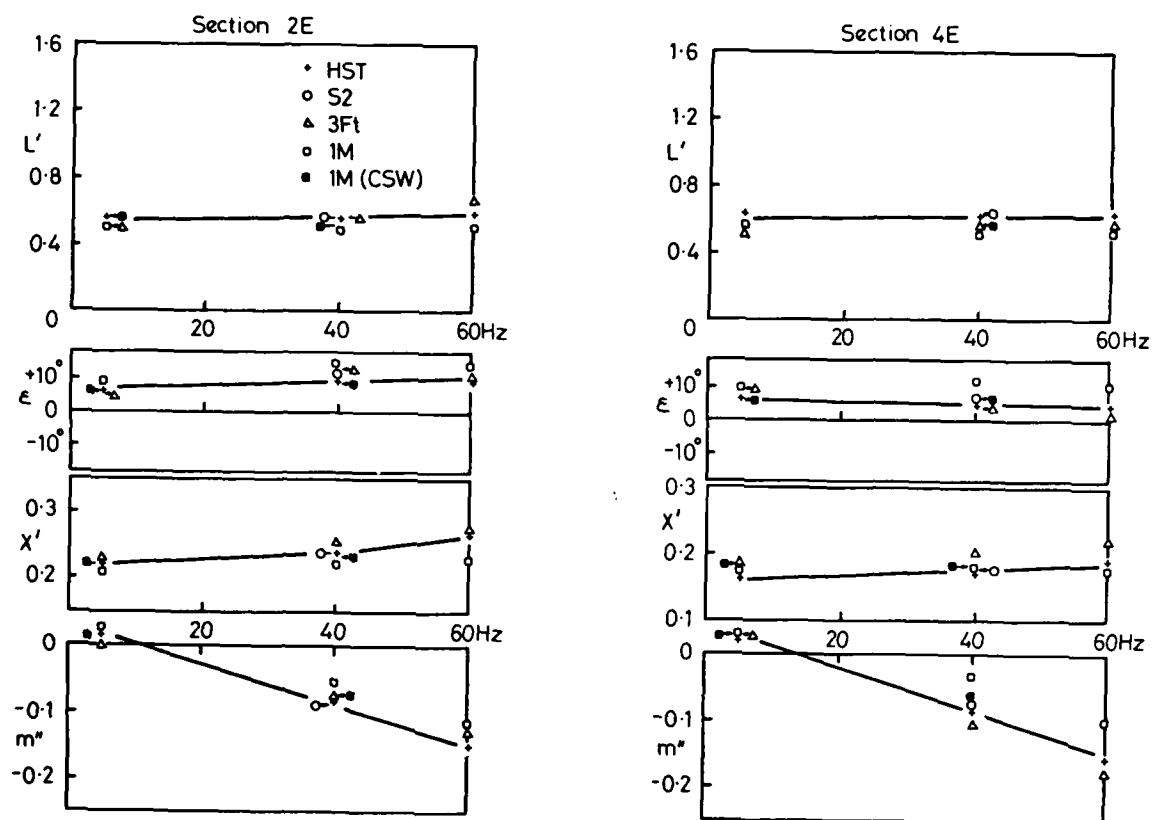
Fig 42   Variation of upper surface chordal properties with frequency.
M = 0.90, α = 0.

43
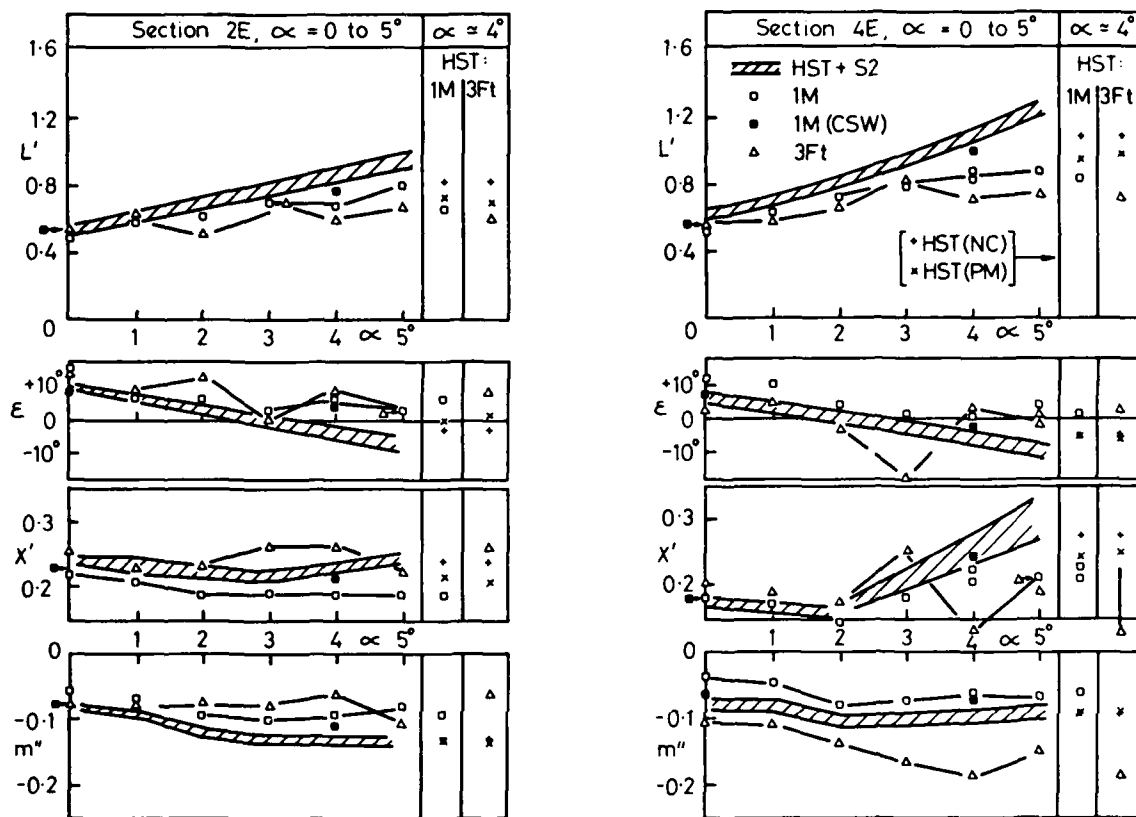
Fig 43   Variation of upper surface chordal properties with incidence.
M = 0.90, f = 40Hz.

44
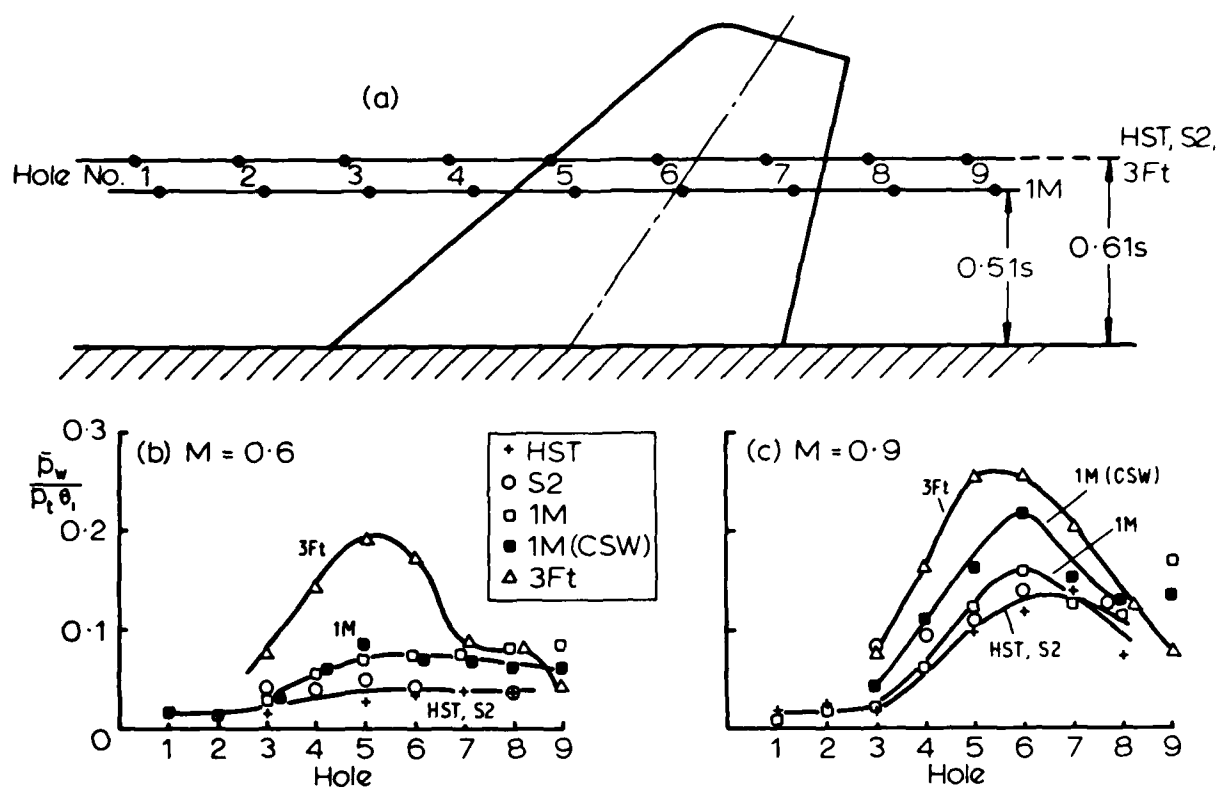
Fig 44   Oscillatory pressures at tunnel roof or floor. $\alpha = 0$, $f = 40$Hz.

REPORT DOCUMENTATION PAGE

13. Keywords/Descriptors

Wind tunnels	Flutter
Wind tunnel tests	Aerodynamic interference
Model tests	Oscillations
Aircraft	

14. Abstract

The European GARTEUR organization initiated, a few years ago, a cooperative programme
on the effects of the walls of a wind tunnel on the behaviour of dynamic models used for
flutter certification of aircraft. Tests have been completed by the same team, on the same
model, in four European wind tunnels and the results, collected in the same form, have
been thoroughly analyzed. The report describes the experiments and presents the most
important results and practical conclusions.

400043

AGARD-R-673

AGARD Report No.673
Advisory Group for Aerospace Research and Development, NATO
COMPARATIVE MEASUREMENTS IN FOUR EUROPEAN WIND TUNNELS OF THE UNSTEADY PRESSURES ON AN OSCILLATING MODEL (THE NORA EXPERIMENTS)
by N.Lambourne, R.Destuynder, K.Kienappel and R.Roos
Published February 1980
48 pages

The European GARTEUR organization initiated, a few years ago, a cooperative programme on the effects of the walls of a wind tunnel on the behaviour of dynamic models used for flutter certification of aircraft. Tests

P.T.O.

Wind tunnels
Wind tunnel tests
Model tests
Aircraft
Flutter
Aerodynamic interference
Oscillations

AGARD-R-673

AGARD Report No.673
Advisory Group for Aerospace Research and Development, NATO
COMPARATIVE MEASUREMENTS IN FOUR EUROPEAN WIND TUNNELS OF THE UNSTEADY PRESSURES ON AN OSCILLATING MODEL (THE NORA EXPERIMENTS)
by N.Lambourne, R.Destuynder, K.Kienappel and R.Roos
Published February 1980
48 pages

The European GARTEUR organization initiated, a few years ago, a cooperative programme on the effects of the walls of a wind tunnel on the behaviour of dynamic models used for flutter certification of aircraft. Tests

P.T.O.

Wind tunnels
Wind tunnel tests
Model tests
Aircraft
Flutter
Aerodynamic interference
Oscillations

AGARD-R-673

AGARD Report No.673
Advisory Group for Aerospace Research and Development, NATO
COMPARATIVE MEASUREMENTS IN FOUR EUROPEAN WIND TUNNELS OF THE UNSTEADY PRESSURES ON AN OSCILLATING MODEL (THE NORA EXPERIMENTS)
by N.Lambourne, R.Destuynder, K.Kienappel and R.Roos
Published February 1980
48 pages

The European GARTEUR organization initiated, a few years ago, a cooperative programme on the effects of the walls of a wind tunnel on the behaviour of dynamic models used for flutter certification of aircraft. Tests

P.T.O.

Wind tunnels
Wind tunnel tests
Model tests
Aircraft
Flutter
Aerodynamic interference
Oscillations

AGARD-R-673

AGARD Report No.673
Advisory Group for Aerospace Research and Development, NATO
COMPARATIVE MEASUREMENTS IN FOUR EUROPEAN WIND TUNNELS OF THE UNSTEADY PRESSURES ON AN OSCILLATING MODEL (THE NORA EXPERIMENTS)
by N.Lambourne, R.Destuynder, K.Kienappel and R.Roos
Published February 1980
48 pages

The European GARTEUR organization initiated, a few years ago, a cooperative programme on the effects of the walls of a wind tunnel on the behaviour of dynamic models used for flutter certification of aircraft. Tests

P.T.O.

Wind tunnels
Wind tunnel tests
Model tests
Aircraft
Flutter
Aerodynamic interference
Oscillations

5274
4

AGARD

NATO ⊕ OTAN

7 RUE ANCELLE · 92200 NEUILLY-SUR-SEINE

FRANCE

Telephone 745.08.10 · Telex 610176

**DISTRIBUTION OF UNCLASSIFIED
AGARD PUBLICATIONS**

AGARD does NOT hold stocks of AGARD publications at the above address for general distribution. Initial distribution of AGARD publications is made to AGARD Member Nations through the following National Distribution Centres. Further copies are sometimes available from these Centres, but if not may be purchased in Microfiche or Photocopy form from the Purchase Agencies listed below.

NATIONAL DISTRIBUTION CENTRES

BELGIUM
Coordonnateur AGARD - VSL
Etat-Major de la Force Aérienne
Quartier Reine Elisabeth
Rue d'Evere, 1140 Bruxelles

CANADA
Defence Science Information Services
Department of National Defence
Ottawa, Ontario K1A OK2

DENMARK
Danish Defence Research Board
Østerbrogades Kaserne
Copenhagen Ø

FRANCE
O.N.E.R.A. (Direction)
29 Avenue de la Division Leclerc
92320 Châtillon sous Bagneux

GERMANY
Zentralstelle für Luft- und Raumfahrt-
dokumentation und -information
c/o Fachinformationszentrum Energie,
Physik, Mathematik GmbH
Kernforschungszentrum
7514 Eggenstein-Leopoldshafen 2

GREECE
Hellenic Air Force General Staff
Research and Development Directorate
Holargos, Athens

ICELAND
Director of Aviation
c/o Flugrad
Reykjavik

ITALY
Aeronautica Militare
Ufficio del Delegato Nazionale all'AGARD
3, Piazzale Adenauer
Roma/EUR

LUXEMBOURG
See Belgium

NETHERLANDS
Netherlands Delegation to AGARD
National Aerospace Laboratory, NLR
P.O. Box 126
2600 A.C. Delft

NORWAY
Norwegian Defence Research Establishment
Main Library
P.O. Box 25
N-2007 Kjeller

PORTUGAL
Direcção do Serviço de Material
da Forca Aerea
Rua da Escola Politécnica 42
Lisboa
Attn: AGARD National Delegate

TURKEY
Department of Research and Development (ARGE)
Ministry of National Defence, Ankara

UNITED KINGDOM
Defence Research Information Centre
Station Square House
St. Mary Cray
Orpington, Kent BR5 3RF

UNITED STATES
National Aeronautics and Space Administration (NASA)
Langley Field, Virginia 23365
Attn: Report Distribution and Storage Unit

THE UNITED STATES NATIONAL DISTRIBUTION CENTRE (NASA) DOES NOT HOLD
STOCKS OF AGARD PUBLICATIONS, AND APPLICATIONS FOR COPIES SHOULD BE MADE
DIRECT TO THE NATIONAL TECHNICAL INFORMATION SERVICE (NTIS) AT THE ADDRESS BELOW.

PURCHASE AGENCIES

Microfiche or Photocopy

National Technical
Information Service (NTIS)
5285 Port Royal Road
Springfield
Virginia 22161, USA

Microfiche

Space Documentation Service
European Space Agency
10, rue Mario Nikis
75015 Paris, France

Microfiche

Technology Reports
Centre (DTI)
Station Square House
St. Mary Cray
Orpington, Kent BR5 3RF
England

Requests for microfiche or photocopies of AGARD documents should include the AGARD serial number, title, author or editor, and publication date. Requests to NTIS should include the NASA accession report number. Full bibliographical references and abstracts of AGARD publications are given in the following journals:

Scientific and Technical Aerospace Reports (STAR)
published by NASA Scientific and Technical
Information Facility
Post Office Box 8757
Baltimore Washington International Airport
Maryland 21240, USA

Government Reports Announcements (GRA)
published by the National Technical
Information Services, Springfield
Virginia 22161, USA